



ONE-PARAMETER BIFURCATIONS IN PLANAR FILIPPOV SYSTEMS

YU. A. KUZNETSOV*, S. RINALDI and A. GRAGNANI†

**Institute of Mathematical Problems in Biology, Pushchino,
Moscow Region, 142292 Russia*

*Mathematisch Instituut, Universiteit Utrecht,
Boedapestlaan 6, 3584 CD Utrecht, The Netherlands*

†*Dipartimento di Elettronica e Informazione, Politecnico di Milano,
Via Ponzio 34/5, 20133 Milano, Italy*

Received March 28, 2002; Revised June 11, 2002

We give an overview of all codim 1 bifurcations in generic planar discontinuous piecewise smooth autonomous systems, here called Filippov systems. Bifurcations are defined using the classical approach of topological equivalence. This allows the development of a simple geometric criterion for classifying sliding bifurcations, i.e. bifurcations in which some sliding on the discontinuity boundary is critically involved. The full catalog of local and global bifurcations is given, together with explicit topological normal forms for the local ones. Moreover, for each bifurcation, a defining system is proposed that can be used to numerically compute the corresponding bifurcation curve with standard continuation techniques. A problem of exploitation of a predator–prey community is analyzed with the proposed methods.

Keywords: Discontinuous piecewise smooth systems; Filippov systems; sliding bifurcations; continuation techniques.

1. Introduction

Piecewise smooth systems (PSS) are described by a finite set of ODEs

$$\dot{x} = f^{(i)}(x), \quad x \in S_i \subset \mathbf{R}^n, \quad (1)$$

where S_i , $i = 1, 2, \dots, m$, are open nonoverlapping regions separated by $(n - 1)$ -dimensional submanifolds (boundaries). The functions $f^{(i)}$ and the boundaries are supposed to be smooth and the union of all the boundaries Σ and all S_i together cover the entire state space.

PSS are frequently encountered in all fields of science and engineering, where relationships among relevant variables are smooth but can be of different nature in some regions of state space. Among the most famous examples of PSS, there are stick-slip mechanical systems, where the friction between two surfaces is nonzero and changes sign with the relative velocity of the surfaces [Galvanetto *et al.*,

1995; Van de Vrande *et al.*, 1999]. But nonsmooth mechanics [Brogliato, 1999] include many other important applications as rocking blocks [Hogan, 1989], suspension bridges [Doole & Hogan, 1996], vibrations and noise [Oestreich *et al.*, 1997], and robotics [McGeer, 1990]. Electrical and electronic devices are systematically modeled as PSS whenever they contain diodes and transistors [Hasler & Neiryneck, 1985; di Bernardo *et al.*, 1998]. Moreover, PSS have a long tradition in process control theory [Flügge-Lotz, 1953; Utkin, 1977; Tsytkin, 1984] where they are used to model on–off feedback control systems. Finally, interesting problems concerning PSS can be formulated also in economics, medicine and biology. One of these problems, dealing with the conflict between conservation and exploitation of natural resources, is shortly discussed in the example presented at the end of the paper.

PSS are called *continuous* if $f^{(i)}(x) = f^{(j)}(x)$ at any point of the boundary Σ_{ij} separating two adjacent regions S_i and S_j . In these systems the vector \dot{x} is uniquely defined at any point of the state space and orbits in region S_i approaching transversally the boundary Σ_{ij} , cross it and enter into the adjacent region S_j . By contrast, in *discontinuous* PSS (from now on called *Filippov systems*), two different vectors \dot{x} , namely $f^{(i)}(x)$ and $f^{(j)}(x)$, can be associated to a point $x \in \Sigma_{ij}$. If the transversal components of $f^{(i)}(x)$ and $f^{(j)}(x)$ have the same sign, the orbit crosses the boundary and has, at that point, a discontinuity in its tangent vector. On the contrary, if the transversal components of $f^{(i)}(x)$ and $f^{(j)}(x)$ are of opposite sign, i.e. if the two vector fields are “pushing” in opposite directions, the state of the system is forced to remain on the boundary and slide on it. Although, in principle, motions on the boundary could be defined in different ways, the most natural one is *Filippov convex method* [Filippov, 1964, 1988] that defines *sliding motions* on Σ_{ij} as the solutions on Σ_{ij} of the continuous ODE $\dot{x} = g(x)$, where $g(x)$ is a convex combination of $f^{(i)}(x)$ and $f^{(j)}(x)$ tangent to Σ_{ij} at x . Generically, this convex combination is unique. Thus, the state portrait of a Filippov system is composed of the sliding state portrait on Σ and of the standard state portraits in each region S_i .

Bifurcation analysis of PSS has received a lot of attention in the last years. In most cases, however, the study was restricted to continuous PSS or to bifurcations of Filippov systems not involving sliding [Feigin, 1994; Freire et al., 1998; di Bernardo et al., 1999; di Bernardo et al., 2001]. This greatly simplifies the analysis, since, as we will see in a moment, sliding bifurcations are many and of quite subtle nature. Indeed, the appearance or disappearance of sliding at a particular parameter value is a bifurcation, even if it leaves the attractors of the system unchanged.

As noticed in [Leine, 2000], there is no general agreement on what a bifurcation could be in Filippov systems. This is an unfortunate situation because the comparison between different contributions becomes difficult, if not impossible. Surprisingly, even in the special case of planar systems only local bifurcations have been considered. The first attempt was due to Bautin and Leontovich [1976] who, however, gave an incomplete classification, since they did not allow for sliding. Next major

contribution was due to Filippov [1988], who classified singular points in planar discontinuous systems and identified all codim 1 local singularities. However, some unfoldings of local singularities are missing in Filippov’s work and bifurcations of sliding cycles are not treated at all. Actually, the existing contributions on sliding bifurcations of cycles refer either to specific bifurcations [di Bernardo et al., 1998] or to particular classes of systems, like mechanical systems of the stick-slip type [Galvanetto et al., 1995; Kunze & Küpper 1997, 1997; Leine, 2000; Dankowitz & Nordmark, 2000] and piecewise linear systems [di Bernardo et al., 2001; Kowalczyk & di Bernardo, 2001; Giannakopoulos & Pliete, 2001]. Finally, very little is known on normal forms and on numerical analysis of sliding bifurcations.

For all these reasons, we present a review with reference, however, to the simplest class of Filippov systems, namely generic planar systems. There are 3 merits of the paper. First, bifurcations and their codimensions are defined, as in [Filippov, 1988], using the classical approach of topological equivalence [Bautin & Leontovich, 1976; Guckenheimer & Holmes, 1983; Kuznetsov, 1998]. This allows us to develop a nice geometrical criterion for defining and classifying sliding bifurcations, i.e. bifurcations in which some sliding on the discontinuity boundary is critically involved. Secondly, using this criterion, we derive the full catalog of the codim 1 local and global sliding bifurcations, giving explicit topological normal forms for all local ones. Lastly, for each bifurcation we propose a defining system that can be used to numerically compute the corresponding bifurcation curve using standard continuation techniques [Doedel & Kernévez, 1986; Kuznetsov & Levitin, 1995–1997]. An interesting problem of renewable resources management is solved to show the power of the presented methods. Some comments on the possibility of extending the analysis to higher order systems and to higher codimension sliding bifurcations are given at the end of the paper.

2. Preliminaries

We now consider generic planar Filippov systems and assume, for simplicity, that there are only two regions S_i , i.e.

$$\dot{x} = \begin{cases} f^{(1)}(x), & x \in S_1, \\ f^{(2)}(x), & x \in S_2. \end{cases} \quad (2)$$

Moreover, the discontinuity boundary Σ separating the two regions is described as

$$\Sigma = \{x \in \mathbf{R}^2 : H(x) = 0\},$$

where H is a smooth scalar function with nonvanishing gradient $H_x(x)$ on Σ , and

$$S_1 = \{x \in \mathbf{R}^2 : H(x) < 0\},$$

$$S_2 = \{x \in \mathbf{R}^2 : H(x) > 0\}.$$

The boundary Σ is either closed or goes to infinity in both directions and $f^{(1)} \neq f^{(2)}$ on Σ .

2.1. Standard and sliding solutions

We now briefly recall how solutions of (2) can be constructed by concatenating *standard solutions* in $S_{1,2}$ and *sliding solutions* on Σ obtained with the well-known Filippov convex method (for details, see [Filippov, 1964; Aubin & Cellina, 1984; Filippov, 1988; Kunze, 2000]). Let

$$\sigma(x) = \langle H_x(x), f^{(1)}(x) \rangle \langle H_x(x), f^{(2)}(x) \rangle, \quad (3)$$

where $\langle \cdot, \cdot \rangle$ denotes the standard scalar product. First we define the *crossing set* $\Sigma_c \subset \Sigma$ as

$$\Sigma_c = \{x \in \Sigma : \sigma(x) > 0\}.$$

It is the set of all points $x \in \Sigma$, where the two vectors $f^{(i)}(x)$ have nontrivial normal components of the same sign. By definition, at these points the orbit of (2) crosses Σ , i.e. the orbit reaching x from S_i concatenates with the orbit entering S_j , $j \neq i$, from x .

Then, we define the *sliding set* Σ_s as the complement to Σ_c in Σ , i.e.

$$\Sigma_s = \{x \in \Sigma : \sigma(x) \leq 0\}.$$

The crossing set is open, while the sliding set is the union of closed *sliding segments* and *isolated sliding points*. Points $x \in \Sigma_s$, where

$$\langle H_x(x), f^{(2)}(x) - f^{(1)}(x) \rangle = 0$$

are called *singular sliding points*. At such points, either both vectors $f^{(1)}(x)$ and $f^{(2)}(x)$ are tangent to Σ , or one of them vanishes while the other is tangent to Σ , or they both vanish.

The Filippov method associates the following convex combination $g(x)$ of the two vectors $f^{(i)}(x)$ to each nonsingular sliding point $x \in \Sigma_s$:

$$g(x) = \lambda f^{(1)}(x) + (1 - \lambda) f^{(2)}(x), \quad (4)$$

$$\lambda = \frac{\langle H_x(x), f^{(2)}(x) \rangle}{\langle H_x(x), f^{(2)}(x) - f^{(1)}(x) \rangle}.$$

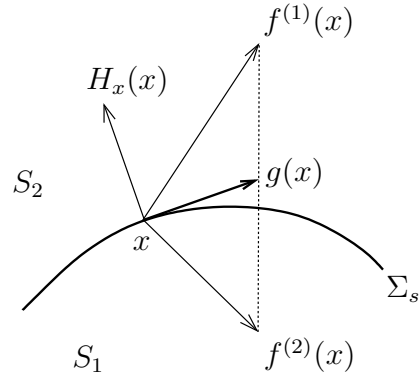


Fig. 1. Filippov construction.

Moreover, excluding infinitely-degenerate cases, $g(x)$ and its derivatives can be defined by continuity at all singular sliding points, which are not isolated sliding points. As indicated in Fig. 1, at nonisolated sliding points $x \in \Sigma_s$

$$\langle H_x(x), g(x) \rangle = 0,$$

i.e. $g(x)$ is tangent to sliding segments of Σ_s . We set $g(x) = 0$ at isolated singular sliding points.

Thus,

$$\dot{x} = g(x), \quad x \in \Sigma_s, \quad (5)$$

defines a scalar differential equation on Σ_s , which is smooth on one-dimensional sliding intervals of Σ_s . Solutions of this equation are called *sliding solutions*.

Special attention should be devoted to equilibria of (5). Notice that, by our setting, all isolated singular sliding points are equilibria of (5). In accordance with [Gatto *et al.*, 1973], equilibria of (5), where the vectors $f^{(i)}(x)$ are transversal to Σ_s and anti-collinear, are called *pseudo-equilibria* of (2) (they are called *quasi-equilibria* in [Filippov, 1988]). This implies that a pseudo-equilibrium P is an internal point of a sliding segment. An equilibrium X of (5), where one of the vectors $f^{(i)}(X)$ vanishes, is called a *boundary equilibrium*.

A sliding segment is delimited either by a boundary equilibrium X , or by a point T (called *tangent point*) where the vectors $f^{(i)}(T)$ are nonzero but one of them is tangent to Σ . Dealing only with generic systems, we can exclude that equilibria of (5) and tangent points accumulate in Σ .

Generically, the sliding segment is either stable or unstable in the normal direction. Indeed, if

$$\langle H_x(x), f^{(1)}(x) \rangle > 0, \quad \langle H_x(x), f^{(2)}(x) \rangle < 0,$$

the sliding segment is stable, while for

$$\langle H_x(x), f^{(1)}(x) \rangle < 0, \quad \langle H_x(x), f^{(2)}(x) \rangle > 0,$$

it is unstable.

It is now possible to define a unique forward solution of (2). For this, assume that $x(0) \in S_1$ and construct the forward solution $x(t)$ of (2) by solving the corresponding equation in S_1 . If this solution does not remain in S_1 , it reaches the boundary Σ at time t_1 , i.e. $H(x(t_1)) = 0$. At this point, there are two possibilities:

(A) If $\sigma(x(t_1)) > 0$, i.e. $x(t_1) \in \Sigma_c$, then we switch to $\dot{x} = f^{(2)}(x)$, and we integrate this equation in region S_2 for $t \geq t_1$. In other words, the orbit crosses Σ at $x(t_1)$.

(B) If $\sigma(x(t_1)) \leq 0$, i.e. $x(t_1) \in \Sigma_s$, then we switch to Eq. (5) on Σ_s thus following a *sliding orbit*. This orbit degenerates to a point if $g(x(t_1)) = 0$, i.e. $x(t_1)$ is an equilibrium of (5). In this case, we set $x(t) = x(t_1)$ for all $t > t_1$. If $g(x(t_1)) \neq 0$, we determine whether a sliding orbit starts at $x(t_1)$ and, if so, we follow the sliding solution $x(t)$ for some $t > t_1$. This solution can remain strictly inside the sliding segment forever (tending toward a pseudo-equilibrium or a singular sliding point with $g = 0$). Alternatively, it can arrive at time $t_2 > t_1$ to its boundary (i.e. to a boundary equilibrium or a tangent point). In the case of the boundary equilibrium, we set $x(t) = x(t_2)$ for all $t > t_2$, while from the tangent point we follow the unique standard orbit in S_1 or S_2 that departs from $x(t_2)$.

The same procedure can be applied to the reversed system (2), with $f^{(i)}(x) \mapsto -f^{(i)}(x)$, to generate a unique backward solution. Although the solutions are uniquely defined both forward and backward in time, system (2) is not invertible in the classical sense, since its orbits can overlap. It should also be pointed out that unstable sliding segments will not be observed in numerical integration of (2).

We note that it is common in the literature to introduce a *differential inclusion* corresponding to a Filippov system (2) and then consider its solutions [Aubin & Cellina, 1984; Filippov, 1988]. This approach, though attractive theoretically, leads to the nonuniqueness of solutions and makes it difficult to define state portraits even in the planar case. Therefore, we do not use differential inclusions in this paper.

2.2. Tangent points

Suppose that a tangent point $T \in \Sigma_s$ is characterized by

$$\langle H_x(T), f^{(1)}(T) \rangle = 0.$$

We say that this tangent point is *visible* (*invisible*) if the orbit of $\dot{x} = f^{(1)}(x)$ starting at T belongs to S_1 (S_2) for all sufficiently small $|t| \neq 0$. Similar definitions hold for the vector field $f^{(2)}$.

Suppose $T = (0, 0)$ and assume that the discontinuity boundary Σ is locally given by the equation $x_2 = 0$, i.e. $H(x) = x_2$. If this is not the case, one can always translate the origin of coordinates to T and then introduce new coordinates (y_1, y_2) by the following construction. Introduce any smooth local parameterization y_1 of Σ near the origin (with $y_1 = 0$ corresponding to T) and consider orbits of the gradient system

$$\dot{x} = H_x(x).$$

Since $H(x)$ is smooth and $H_x(T) \neq 0$, this system is smooth and its orbits cross Σ orthogonally near T . Assign to any point x near T the y_1 -value at the intersection with Σ of the orbit of the gradient system passing through x . Next, set $y_2 = H(x)$. This defines a local diffeomorphism $x \mapsto y$ near T .

A tangent point T of $f^{(1)}$ is called *quadratic* if the orbit passing through T can be locally represented as $x_2 = (1/2)\nu_1 x_1^2 + O(x_1^3)$, $\nu_1 \neq 0$. Under the above assumptions,

$$f^{(1)}(x) = \left(\begin{array}{c} p_1 + a_1 x_1 + b_1 x_2 + O(\|x\|^2) \\ c_1 x_1 + d_1 x_2 + \frac{1}{2} q_1 x_1^2 + r_1 x_1 x_2 + \frac{1}{2} s_1 x_2^2 + O(\|x\|^3) \end{array} \right),$$

where $p_1 \neq 0$, and

$$\nu_1 = \frac{c_1}{p_1}.$$

If $\nu_1 < 0$, the tangent point is visible, while if $\nu_1 > 0$ it is invisible. Generically, T is not a tangent point

for $f^{(2)}$, so that $f^{(2)}(T)$ is transversal to Σ , as well as all nearby vectors $f^{(2)}(x)$, $x \in \Sigma$. This implies that in a neighborhood of a generic tangent point the orbits are like in Figs. 2(a) and 2(b) (with a

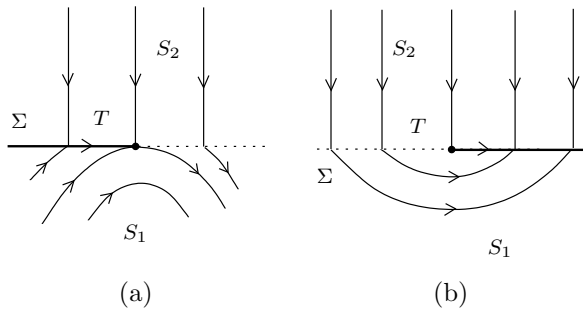


Fig. 2. Generic (a) visible and (b) invisible tangent point. The thick orbit is a sliding orbit.

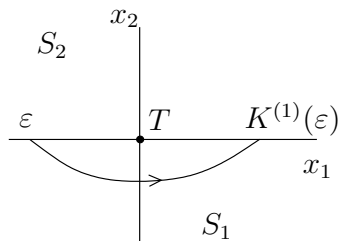


Fig. 3. Map $K^{(1)}$.

possible reversal of all arrows and/or reflection with respect to the vertical axis).

Near an invisible tangent point, a useful map

$$\varepsilon \mapsto K^{(1)}(\varepsilon), \quad \varepsilon \in \mathbf{R}, \tag{6}$$

can be defined along the orbits of $f^{(1)}$ (see Fig. 3). When $p_1 > 0$ (as in Fig. 3), the map is defined for $\varepsilon < 0$. On the contrary, when $p_1 < 0$, the map is defined for $\varepsilon > 0$. Let us consider only the case $p_1 > 0$. As shown in [Filippov, 1988] (see also [Gubar', 1971]), map (6) is smooth near a quadratic invisible tangent point and has the expansion

$$K^{(1)}(\varepsilon) = -\varepsilon + k_2^{(1)}\varepsilon^2 + O(\varepsilon^3),$$

where

$$k_2^{(1)} = \frac{2}{3} \left(\frac{a_1 + d_1}{p_1} - \frac{q_1}{2c_1} \right).$$

Map (6) is particularly important for the analysis of a singular pseudo-equilibrium, called *fused focus*, where an invisible tangent point of $f^{(1)}$ coincides with an invisible tangent point of $f^{(2)}$ (see Sec. 3.2.4 below). This is an isolated singular sliding point, where the Filippov vector $g = 0$ by definition. In this case, a Poincaré map P can be constructed by composing $K^{(1)}$ (defined for $\varepsilon < 0$) and $K^{(2)}$

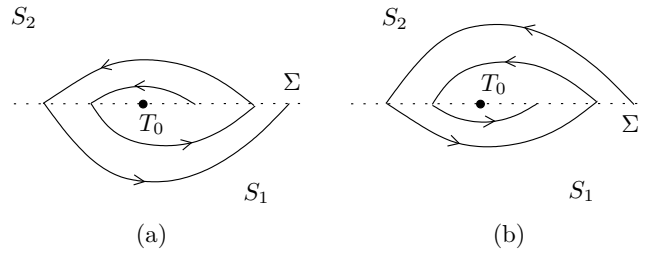


Fig. 4. (a) Unstable and (b) stable fused focus.

(defined for $\varepsilon > 0$). When both invisible tangent points are quadratic, this gives

$$P(\varepsilon) = \varepsilon + (k_2^{(1)} - k_2^{(2)})\varepsilon^2 + O(\varepsilon^3)$$

for $\varepsilon < 0$, so that the fused focus is locally stable if

$$k_2 = k_2^{(1)} - k_2^{(2)} < 0,$$

and unstable if $k_2 > 0$ (see Fig. 4). As we shall see, k_2 plays a role similar to that of the first Lyapunov coefficient in the analysis of Hopf bifurcations [Kuznetsov, 1998]. It should be noted that a fused focus, which is not an equilibrium of $f^{(1)}$ or $f^{(2)}$, should not be confused with the so-called *focus-focus* boundary equilibrium [Bautin & Leontovich, 1976; Kunze, 2000].

2.3. Topological equivalence and bifurcations

The *state portrait* of (2) is the union of all its orbits in \mathbf{R}^2 . As already mentioned, these orbits can overlap when sliding. Two Filippov systems of the form (2) are *topologically equivalent* if there is a homeomorphism $h: \mathbf{R}^2 \rightarrow \mathbf{R}^2$ that maps the state portrait of one system onto the state portrait of the other, preserving orientation of the orbits. Notice that all sliding segments of one system are mapped onto sliding segments of the other. Moreover, we require that h maps the discontinuity boundary Σ of one system onto the discontinuity boundary of the other system.

Now consider a Filippov system depending on a parameter (a *one-parameter family*):

$$\dot{x} = \begin{cases} f^{(1)}(x, \alpha), & x \in S_1(\alpha), \\ f^{(2)}(x, \alpha), & x \in S_2(\alpha), \end{cases} \tag{7}$$

where $x \in \mathbf{R}^2$, $\alpha \in \mathbf{R}$, and $f^{(i)}$, $i = 1, 2$, are smooth functions of (x, α) , while

$$S_1(\alpha) = \{x \in \mathbf{R}^2 : H(x, \alpha) < 0\},$$

$$S_2(\alpha) = \{x \in \mathbf{R}^2 : H(x, \alpha) > 0\},$$

for some smooth function $H(x, \alpha)$ with $H_x(x, \alpha) \neq 0$ for all (x, α) such that $H(x, \alpha) = 0$.

We say that (7) exhibits a *bifurcation* at $\alpha = \alpha_0$ if by an arbitrarily small parameter perturbation we get a topologically nonequivalent system.

Recall that a bifurcation has codim 1 if it appears at isolated parameter values in generic one-parameter families. All bifurcations of (7) can be classified as *local* or *global*. A local bifurcation can be detected by looking at a fixed but arbitrarily small neighborhood of a point in the plane. All other bifurcations will be called *global* in this paper. Under this definition, all bifurcations involving nonvanishing cycles are classified as global bifurcations. Of course, we do not consider bifurcations occurring in regions S_1 or S_2 , but focus only on codim 1 bifurcations which involve sliding on the discontinuity boundary. Actually, the appearance or disappearance of a sliding segment is already a bifurcation, since a state portrait with overlapping orbits cannot be homeomorphically transformed into a state portrait without overlappings.

To produce all generic one-parameter bifurcations involving the discontinuity boundary Σ , we use the following classification criterion. For a given parameter value α , consider the sliding set $\Sigma_s \subset \Sigma$ and find all pseudo-equilibria and tangent points in it. In view of our genericity assumption, these points are in finite number but can collide when α varies, leading to local codim 1 bifurcations. Another local codim 1 bifurcation occurs when a standard hyperbolic equilibrium in S_1 or S_2 approaches the boundary Σ and “hits” it for some parameter value. Obviously, there are no other local codim 1 bifurcations. To detect global codim 1 bifurcations involving sliding, consider the so-called *special orbits*, namely the orbits entering S_1 or S_2 from pseudo-equilibria or tangent points. A bounded special orbit can return in finite time to the sliding set Σ_s or tend asymptotically to its ω -limit set. The return points vary with α and could “collide” with pseudo-equilibria or tangent points in Σ_s for some parameter value. Such collisions imply global bifurcations. Generically, an ω -limit set of a special orbit is a stable standard equilibrium or a cycle (which can cross Σ). Collisions of equilibria with the discontinuity boundary have already been taken into account. Thus, the remaining possibility is that a nonvanishing cycle hits the sliding set Σ_s . Finally, a global bifurcation can also occur when a special orbit approaches an incoming separatrix of a stan-

dard saddle in S_1 or S_2 and coincides with it at some parameter value.

The advantage of the outlined classification criterion is that it does not capture global bifurcations which are completely analogous to their smooth counterparts, namely those bifurcations in which critical orbits cross the discontinuity boundary several times but do not slide.

3. Local Bifurcations

In this section we summarize results on local bifurcations in one-parameter Filippov systems (7). For each bifurcation, we give (without proof) a so-called *topological normal form*, i.e. a polynomial Filippov system such that any generic Filippov system satisfying the same bifurcation condition is locally topologically equivalent to it.

3.1. Collisions of equilibria with the boundary

Suppose that a hyperbolic equilibrium X_α of $\dot{x} = f^{(1)}(x, \alpha)$ exists in S_1 for $\alpha < 0$ and collides at $\alpha = 0$ with the discontinuity boundary Σ . Moreover, assume that X_α has simple eigenvalues and hits Σ with a nonzero velocity with respect to the parameter at a point X_0 , where $f^{(2)}(x, \alpha)$ is transversal to Σ . This happens in generic one-parameter families of planar Filippov systems. Without loss of generality, we can assume that Σ is locally a straight line and that $f^{(2)}$ is orthogonal to Σ in a neighborhood of X_0 for small α . Indeed, after introducing a smooth scalar parameterization y_1 of Σ with $y_1 = 0$ corresponding to X_0 , one can take as the second coordinate of a point x the value $y_2 = H(x, \alpha)$ of the function defining Σ , and as the first coordinate the value y_1 at the intersection of the discontinuity boundary Σ with the orbit of $f^{(2)}$ passing through x . In the y -coordinates the discontinuity boundary is given by $y_2 = 0$, while the orbits of $f^{(2)}$ are straight lines $y_1 = \text{const}$. The map $x \mapsto y$ is a local diffeomorphism that depends smoothly on α . The system $\dot{x} = f^{(1)}(x, \alpha)$ written in the y -coordinates will obviously have a hyperbolic equilibrium colliding with the discontinuity boundary.

3.1.1. Boundary focus

Assume that the colliding focus is *unstable* and has *counter-clockwise rotation* nearby (the case of a stable and/or clockwise focus can be immediately understood by reversing all arrows in the figures

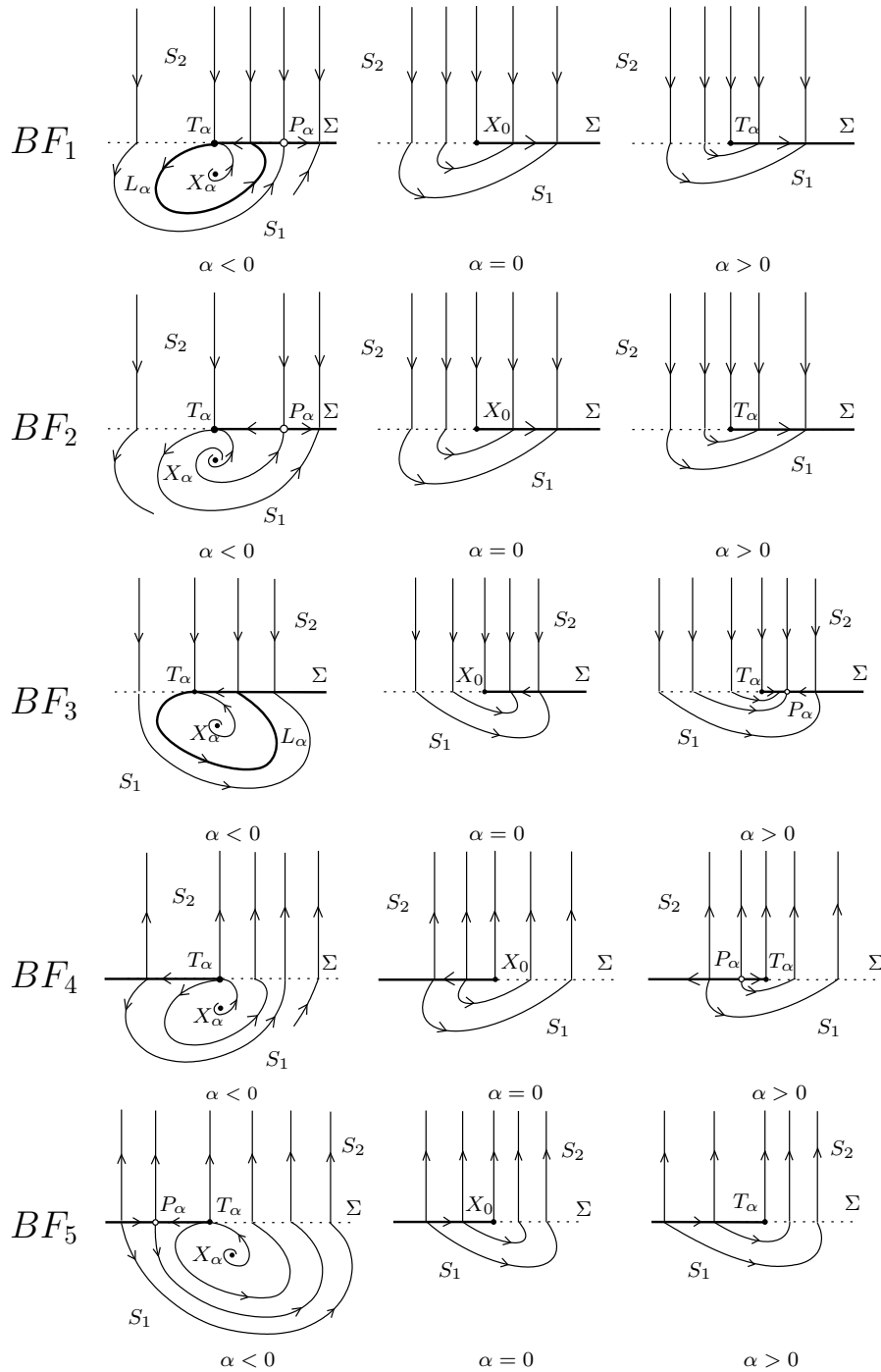


Fig. 5. Boundary focus bifurcations: In cases BF_1 and BF_3 stable sliding cycles exist for nearby parameter values.

and/or by reflecting the figures with respect to the vertical axis).

There are five generic critical cases: BF_i , $i = 1, 2, 3, 4, 5$. In all cases, there is a visible tangent point when $\alpha < 0$, and an invisible tangent point when $\alpha > 0$. The cases are distinguished by the relative position of the focus zero-isoclines and the

behavior of the orbit departing from the visible tangent point into S_1 , as well as by the direction of the motion in S_2 .

The unfoldings of these singularities are presented in Fig. 5. In cases BF_1 , BF_2 and BF_3 , there is a *stable sliding orbit* at $\alpha = 0$ that departs from the equilibrium or approaches it. By

contrast, in cases BF_4 and BF_5 , the sliding orbit is unstable.

In case BF_1 , a stable sliding cycle L_α surrounds the unstable focus X_α for $\alpha < 0$. The sliding segment of the cycle ends at the visible tangent point T_α and begins at a transverse arrival point located between T_α and a pseudo-saddle P_α . The domain of attraction of this cycle is bounded by the stable separatrices of P_α . When $\alpha \rightarrow 0$, the stable cycle shrinks, while the three points, X_α, T_α and P_α , collide simultaneously. For small $\alpha > 0$, there are no equilibria or cycles and the stable sliding orbit begins at the invisible tangent point T_α . This bifurcation entails the catastrophic disappearance of a stable sliding cycle.

In case BF_2 , the orbit departing from the visible tangent point T_α for small $\alpha < 0$ returns to Σ at the right of the pseudo-saddle P_α . Thus, no sliding cycle exists. The state portraits for $\alpha = 0$ and $\alpha > 0$ are like in case BF_1 .

Analytically, one can distinguish the cases BF_1 and BF_2 as follows. Let

$$f_x^{(1)}(X_0, 0) = \begin{pmatrix} a & b \\ c & d \end{pmatrix},$$

and consider the positive half-orbit of the planar linear system

$$\begin{cases} \dot{x}_1 = ax_1 + bx_2, \\ \dot{x}_2 = cx_1 + dx_2, \end{cases}$$

that departs from point T on the line $x_2 = 1$ where $\dot{x}_2 = 0$, i.e.

$$T = \left(-\frac{d}{c}, 1 \right).$$

This orbit makes a counter-clockwise excursion, and returns to the same line $x_2 = 1$ at point $R = (\theta, 1)$. Case BF_1 corresponds to

$$\theta < -\frac{b}{a},$$

while the opposite inequality characterizes BF_2 . For the critical value

$$\theta = -\frac{b}{a}$$

the orbit is orthogonal to the line $x_2 = 1$ at the point R (see Fig. 6). This corresponds to a codim 2 singularity (*degenerate boundary focus*). It can be shown that this critical value is characterized by

$$\frac{d-a}{2\omega} \operatorname{tg} \left[\frac{\omega}{a+d} \ln \left(-\frac{bc}{a^2} \right) \right] = 1, \quad (8)$$

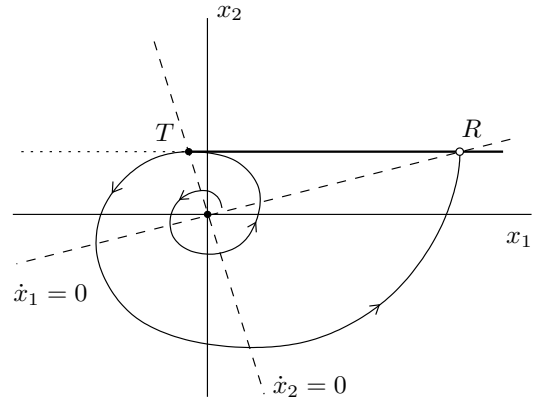


Fig. 6. Degenerate boundary focus.

where

$$\omega = \frac{1}{2} \sqrt{-(a-d)^2 - 4bc}.$$

Note that a related formula on p. 246 in [Filippov, 1988] contains misprints.

In case BF_3 (see Fig. 5 again), a stable sliding cycle L_α passing through the visible tangent point T_α surrounds the unstable focus X_α for $\alpha < 0$. Contrary to case BF_1 , there is no pseudo-equilibrium nearby. When $\alpha \rightarrow 0$, the stable cycle shrinks and the focus X_α collides with the tangent point T_α . For small $\alpha > 0$, there is no cycle and all nearby orbits tend to a stable pseudo-equilibrium P_α that exists close to the invisible tangent point T_α . This bifurcation implies the noncatastrophic disappearance of a stable sliding cycle.

In case BF_4 , the visible tangent point T_α present for small $\alpha < 0$ is the starting point of an unstable sliding orbit. Since the focus is unstable, all orbits leave a small neighborhood of the critical equilibrium. The same is true for $\alpha > 0$ with the only difference that a repelling pseudo-equilibrium P_α exists near the invisible tangent point T_α .

In the last case BF_5 , no attractor exists near the bifurcation, that can be seen as the collision of a pseudo-saddle P_α with the visible tangent point T_α and the focus X_α as $\alpha \rightarrow 0$. After the collision, only an invisible tangent point T_α remains.

One can easily provide topological normal forms for all the above cases. For example, the system

$$\dot{x} = \begin{cases} f^{(1)}(x), & H(x, \alpha) < 0, \\ f^{(2)}(x), & H(x, \alpha) > 0, \end{cases} \quad (9)$$

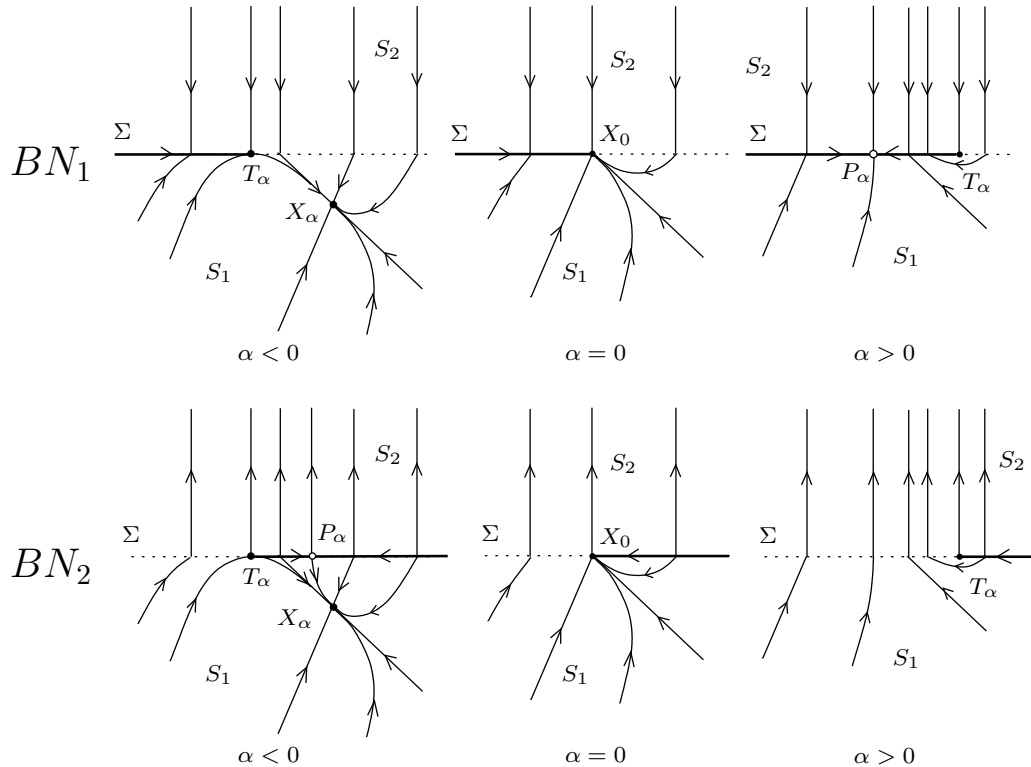


Fig. 7. Boundary node bifurcations.

where

$$f^{(1)}(x) = \begin{pmatrix} x_1 - 2x_2 \\ 4x_1 \end{pmatrix},$$

$$f^{(2)}(x) = \begin{pmatrix} 0 \\ -1 \end{pmatrix}, \quad H(x, \alpha) = x_2 + \alpha,$$

is a normal form for case BF_1 . It is convenient to assume that H depends on the unfolding parameter α , while $f^{(1)}$ and $f^{(2)}$ do not. Notice that by setting

$$f^{(1)}(x) = \begin{pmatrix} x_1 - 2x_2 \\ 3x_1 \end{pmatrix}$$

with $f^{(2)}$ and $H(x, \alpha)$ as above, one obtains case BF_2 , while

$$f^{(1)}(x) = \begin{pmatrix} -x_1 - 2x_2 \\ 4x_1 + 2x_2 \end{pmatrix}$$

corresponds to BF_3 . Normal forms for BF_4 and BF_5 can be obtained from those for BF_2 and BF_3 , respectively, by setting

$$f^{(2)}(x) = \begin{pmatrix} 0 \\ 1 \end{pmatrix}.$$

3.1.2. Boundary node

Assume that the colliding node X_0 is stable. Depending on the direction of the motion in S_2 , there are two generic critical cases. The unfoldings of the singularities $BN_{1,2}$ are presented in Fig. 7. Cases with unstable nodes or nodes with differently inclined zero-isoclines can be reduced to the considered ones. In case BN_1 , the critical equilibrium X_0 is an attractor with an incoming stable sliding orbit. In case BN_2 the equilibrium X_0 is unstable but has a sector of incoming orbits (bounded by the unstable sliding orbit and the nonleading manifold of the node). In both cases, there is a visible tangent point when $\alpha < 0$, and an invisible tangent point when $\alpha > 0$.

In case BN_1 , a stable node X_α and a visible tangent point T_α coexist for $\alpha < 0$. They collide at $\alpha = 0$ and are substituted by a stable pseudo-node P_α and an invisible tangent point T_α for $\alpha > 0$. This bifurcation illustrates how a stable node can become a stable pseudo-node.

In case BN_2 , a pseudo-saddle P_α and the stable node X_α coexist for $\alpha < 0$ with the visible tangent point T_α , while there is only a tangent point T_α for

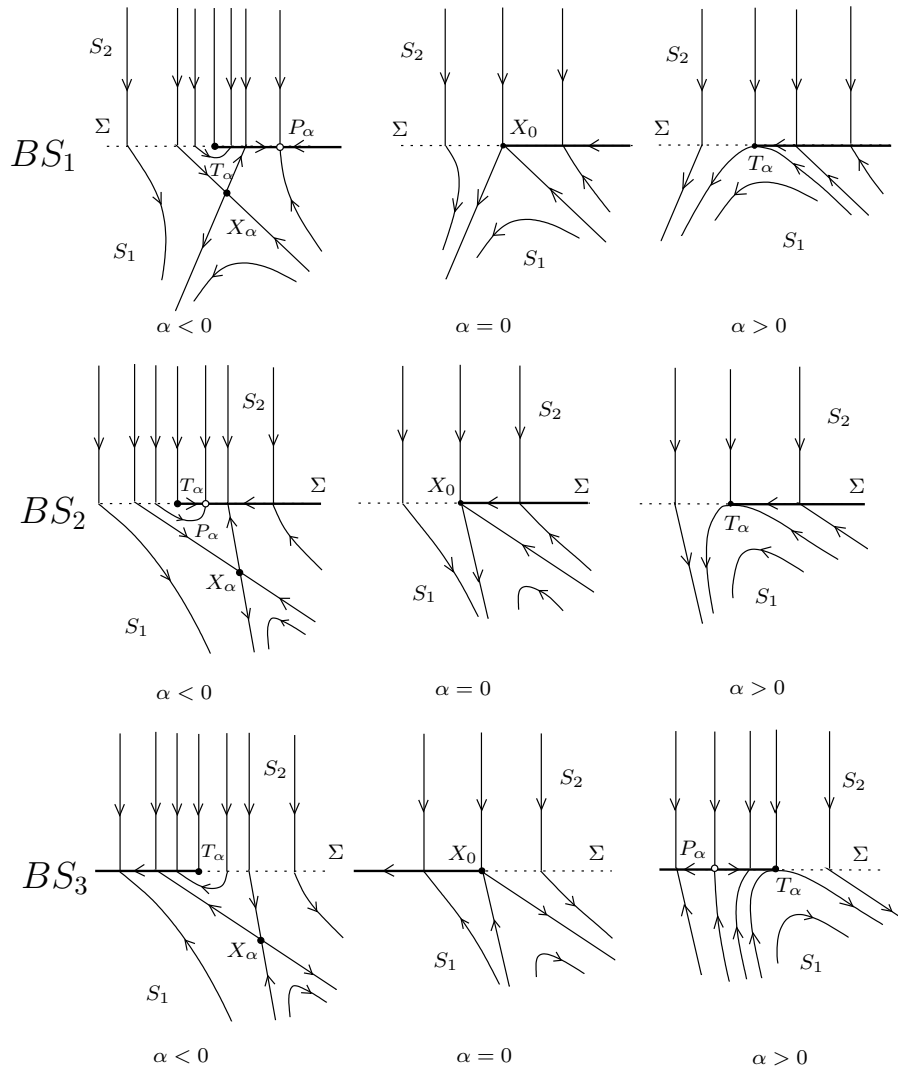


Fig. 8. Boundary saddle bifurcations: In cases BS_1 and BS_2 a stable pseudo-node disappears catastrophically, while a standard saddle becomes a pseudo-saddle in case BS_3 .

$\alpha > 0$. This is a catastrophic disappearance of a stable node.

As in the previous case, it is easy to derive topological normal forms. The normal forms for $BN_{1,2}$ are given by (9) with

$$f^{(1)}(x) = \begin{pmatrix} -3x_1 - x_2 \\ -x_1 - 3x_2 \end{pmatrix},$$

$$f^{(2)}(x) = \begin{pmatrix} 0 \\ \mp 1 \end{pmatrix}, H(x, \alpha) = x_2 + \alpha.$$

3.1.3. Boundary saddle

When the colliding equilibrium is a saddle, there are three generic critical cases (BS_1, BS_2 and BS_3) determined by the slope of the saddle zero-

isoclines. The corresponding unfoldings are presented in Fig. 8. All other cases (i.e. when the saddle is oriented differently or the motion in S_2 is reversed) can be reduced to the considered ones. In all cases, there is an invisible tangent point when $\alpha < 0$, and a visible tangent point when $\alpha > 0$. These points delimit the sliding segments on the discontinuity boundary.

In case BS_1 , a saddle X_α coexists with a pseudo-saddle P_α and an invisible tangent point T_α for $\alpha < 0$. These three points collide at the critical parameter value $\alpha = 0$ and are substituted by a visible tangent point T_α for $\alpha > 0$. No attractor is involved.

In case BS_2 , a saddle X_α coexists with an invisible tangent point T_α and a stable pseudo-node

P_α for $\alpha < 0$, while only a visible tangent point T_α remains for $\alpha > 0$. This is a catastrophic disappearance of a stable pseudo-node.

In the last case BS_3 , for $\alpha < 0$ a saddle X_α coexists with an invisible tangent point T_α , while for $\alpha > 0$, there is a pseudo-saddle P_α and a visible tangent point T_α . This bifurcation shows how a saddle can become a pseudo-saddle.

A topological normal form in case BS_1 , is given by the system (9), where

$$f^{(1)}(x) = \begin{pmatrix} -x_1 + 3x_2 \\ 3x_1 - x_2 \end{pmatrix},$$

$$f^{(2)}(x) = \begin{pmatrix} 0 \\ -1 \end{pmatrix}, H(x, \alpha) = x_2 + \alpha.$$

Normal forms for BS_2 and BS_3 have the same $f^{(2)}$ and H but

$$f^{(1)}(x) = \begin{pmatrix} -2x_1 - x_2 \\ x_1 + x_2 \end{pmatrix}$$

in case BS_2 and

$$f^{(1)}(x) = \begin{pmatrix} x_1 - 3x_2 \\ -3x_1 + x_2 \end{pmatrix}$$

in case BS_3 .

3.2. Collisions of tangent points

If a smooth vector field $f(x, \alpha)$ is quadratically tangent to the boundary Σ at a point T_α , then,

generically, this tangent point will slightly move under parameter variation. In other words, the presence of a quadratic tangent point is not a bifurcation. However, the collision of two tangent points is a local codim 1 bifurcation. Moreover, two tangent points of the same vector field cannot collide if they are both visible or invisible, while tangent points of different vector fields collide independently of their nature. Thus, in generic one-parameter families of planar Filippov systems, one can expect the following critical cases:

- (1) collision of a visible and an invisible tangent point of $f^{(1)}(x, \alpha)$;
- (2) collision of a visible tangent point of $f^{(1)}(x, \alpha)$ and a visible tangent point of $f^{(2)}(x, \alpha)$;
- (3) collision of a visible tangent point of $f^{(1)}(x, \alpha)$ and an invisible tangent point of $f^{(2)}(x, \alpha)$;
- (4) collision of an invisible tangent point of $f^{(1)}(x, \alpha)$ and an invisible tangent point of $f^{(2)}(x, \alpha)$.

In the following, we analyze these possibilities in detail.

3.2.1. Double tangency

Suppose that for $\alpha < 0$ the vector field $f^{(1)}(x, \alpha)$ has two quadratic tangent points: an invisible and a visible one. Let these tangent points collide at $\alpha = 0$ forming a *double tangent point* T_0 . The orbit of $f^{(1)}(x, 0)$ passing through T_0 has generically

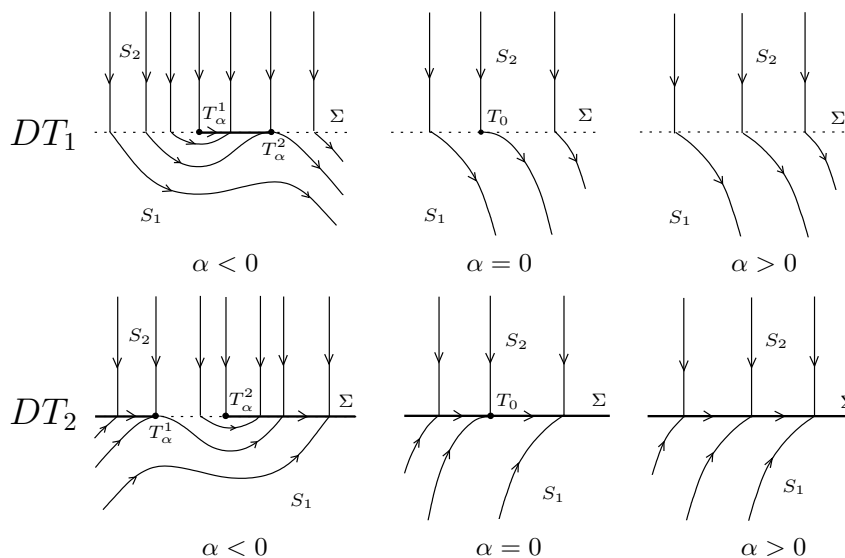


Fig. 9. Double tangency bifurcations. DT_1 : Appearance of a stable sliding segment. DT_2 : Closing of a crossing window.

a *cubic inflection point*. Assume also that $f^{(1)}(x, \alpha)$ is locally transversal to the boundary for $\alpha > 0$ and that the vector field $f^{(2)}$ is transversal to the boundary near T_0 for all small α . As in Sec. 3, we can suppose, without loss of generality, that the boundary Σ is a straight line and that $f^{(2)}$ is orthogonal to Σ .

Under these assumptions, there are two generic critical cases, DT_1 and DT_2 , corresponding to opposite inflections of the orbit passing through T_0 . These critical cases are shown in Fig. 9 together with their unfoldings.

In case DT_1 , a stable sliding segment exists between T_α^1 and T_α^2 for $\alpha < 0$. At the critical value $\alpha = 0$ there is a single orbit that departs from T_0 tangentially to the boundary, while all other orbits cross Σ . For $\alpha > 0$ all orbits cross Σ .

In case DT_2 , there are two stable sliding segments for $\alpha < 0$, separated by a “crossing window” between T_α^1 and T_α^2 . The sliding motions starting on the left segment terminate at T_α^1 and continue in S_1 along a standard orbit that reaches the right sliding segment. At $\alpha = 0$ the crossing window disappears and an uninterrupted sliding orbit exists for $\alpha > 0$.

Topological normal forms for $DT_{1,2}$ are given by (9) with

$$f^{(1)}(x, \alpha) = \begin{pmatrix} 1 \\ \pm(\alpha + x_1^2) \end{pmatrix},$$

$$f^{(2)}(x, \alpha) = \begin{pmatrix} 0 \\ -1 \end{pmatrix}, H(x) = x_2.$$

3.2.2. Two visible tangencies

Now assume that, for all sufficiently small α , $f^{(1)}(x, \alpha)$ has a visible quadratic tangent point $T_\alpha^{(1)} \in \Sigma$, while $f^{(2)}(x, \alpha)$ has a visible quadratic tangent point $T_\alpha^{(2)} \in \Sigma$. Further, suppose that at $\alpha = 0$ these tangent points collide, i.e. $T_0^{(1)} = T_0^{(2)} = T_0$, while their relative velocity with respect to the parameter is nonzero. As before, we can assume that the discontinuity boundary Σ is a straight line. It is easy to see that under these assumptions there are two generic critical cases, VV_1 and VV_2 , in which the vectors $f^{(1)}(T_0, 0)$ and $f^{(2)}(T_0, 0)$ are *collinear* or *anti-collinear*, so that T_0 is a singular sliding point. Figure 10 presents unfoldings of these singularities, assuming that $T_\alpha^{(1)}$ is located to the right of $T_\alpha^{(2)}$ for $\alpha < 0$ and to the left for $\alpha > 0$.

For $\alpha = 0$, in case VV_1 there is a sliding segment containing the singular sliding point, while in case VV_2 only one singular sliding point is present.

In case VV_1 , the tangent points $T_\alpha^{(1)}$ and $T_\alpha^{(2)}$ delimit a segment of Σ which is crossed by orbits going from S_1 to S_2 when $\alpha < 0$, and in the opposite direction when $\alpha > 0$.

In case VV_2 , the tangent points $T_\alpha^{(1)}$ and $T_\alpha^{(2)}$ delimit a stable sliding segment containing a pseudo-saddle P_α for small $\alpha \neq 0$.

Topological normal forms for cases $VV_{1,2}$ are given by (9) with

$$f^{(1)}(x, \alpha) = \begin{pmatrix} \pm 1 \\ \mp(\alpha + x_1) \end{pmatrix},$$

$$f^{(2)}(x, \alpha) = \begin{pmatrix} 1 - x_1 \\ x_1 \end{pmatrix}, H(x) = x_2.$$

3.2.3. One visible and one invisible tangency

When one of the colliding quadratic tangent points (say $T_\alpha^{(1)}$) is invisible, while the other ($T_\alpha^{(2)}$) is visible, there are three generic critical cases: Case VI_1 , when the vectors $f^{(1)}(T_0, 0)$ and $f^{(2)}(T_0, 0)$ are collinear, and two cases (VI_2 and VI_3), when they are anti-collinear. The unfoldings of these three singularities are shown in Fig. 11.

In case VI_1 , all orbits, except one, cross Σ for $\alpha = 0$. The cases VI_2 and VI_3 can be distinguished by looking for $\alpha = 0$ at the coefficient ν_i of the quadratic term in the functions representing the orbit of $f^{(i)}$, $i = 1, 2$, passing through T_0 (see Sec. 2.2). In case VI_2 the orbits in S_1 are less bent than those in S_2 , while the opposite is true in case VI_3 . This results in sliding motions in the opposite directions. Notice, however, that the sliding segment is stable on one side of T_0 and unstable on the other.

Similar to the previous cases, unfolding of case VI_1 gives a sliding segment bounded by the tangent points $T_\alpha^{(1)}$ and $T_\alpha^{(2)}$ for both $\alpha > 0$ and $\alpha < 0$. However, this sliding segment is unstable for $\alpha < 0$ and stable for $\alpha > 0$. Unfolding of cases VI_2 and VI_3 opens a crossing window between $T_\alpha^{(1)}$ and $T_\alpha^{(2)}$ in the sliding segment. In both cases, there are disjoint sliding segments of opposite stability for $\alpha \neq 0$. Moreover, in case VI_2 , there exists a pseudo-saddle for any small $\alpha \neq 0$, while in case VI_3 an unstable pseudo-node existing for $\alpha < 0$ is substituted by a stable pseudo-node for $\alpha > 0$. In other words, approaching the bifurcation from positive values of

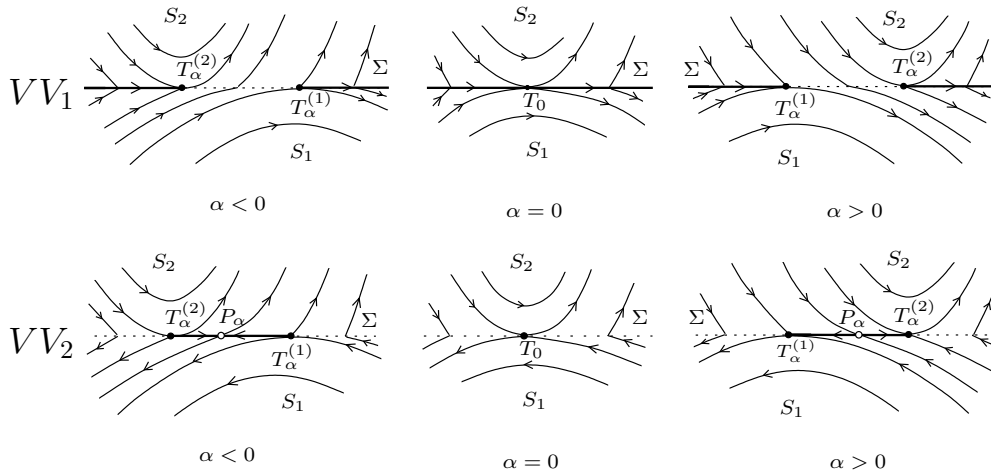


Fig. 10. Collisions of two quadratic tangencies when both tangent points are visible. VV_1 : Closing and opening of a crossing window. VV_2 : Appearance of a stable sliding segment.

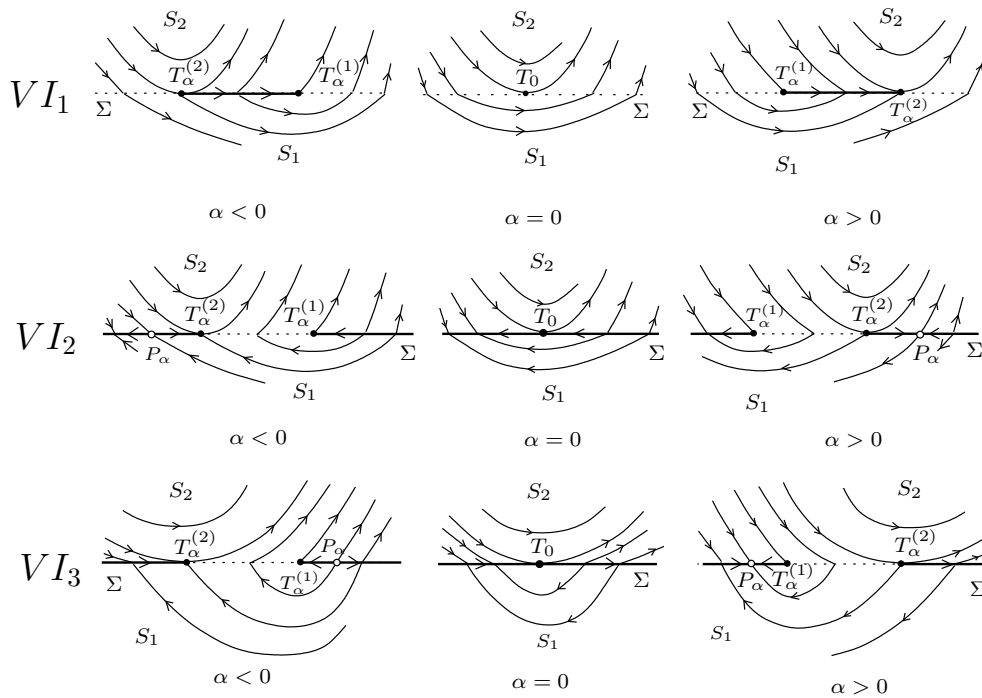


Fig. 11. Collisions of visible and invisible tangencies.

α , we get a catastrophic disappearance of a stable pseudo-equilibrium.

Topological normal forms for cases VI_j are given by (9) with $H(x) = x_2$ and the following $f^{(k)}$. For $VI_{1,2}$:

$$f^{(1)}(x, \alpha) = \begin{pmatrix} \pm 1 - x_1 \\ \pm(\alpha + x_1) \end{pmatrix}, \quad f^{(2)}(x, \alpha) = \begin{pmatrix} 1 - x_1 \\ 2x_1 \end{pmatrix},$$

and for VI_3 :

$$f^{(1)}(x, \alpha) = \begin{pmatrix} -1 + x_1 \\ -\alpha - 2x_1 \end{pmatrix}, \quad f^{(2)}(x, \alpha) = \begin{pmatrix} 1 - x_1 \\ x_1 \end{pmatrix}.$$

3.2.4. Two invisible tangencies

Finally, assume that the two colliding quadratic tangency points are invisible. There are two generic critical cases in which $f^{(1)}$ and $f^{(2)}$ are collinear or

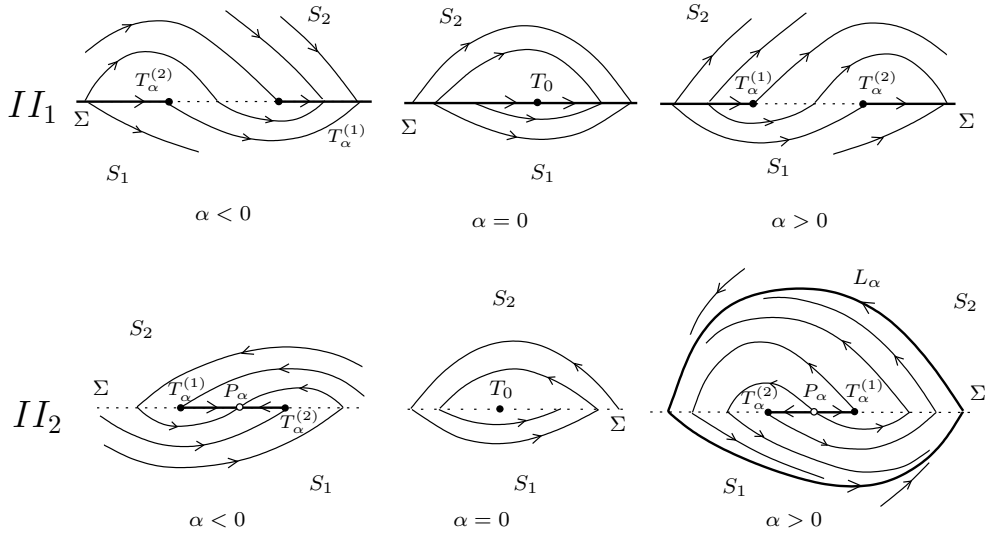


Fig. 12. Collisions of two invisible tangencies.

anti-collinear at the singular sliding point T_0 , respectively (see Fig. 12). In case II_1 , for $\alpha = 0$ there is a sliding segment, on which the sliding is stable on one side of T_0 and unstable on the other. In case II_2 , point T_0 is a fused focus (see Sec. 2.2). Suppose, that the coefficient k_2 defined in Sec. 2.2 is negative. This implies stability of the pseudo-focus. The case of an unstable pseudo-focus can be understood by reversing all arrows in the portraits.

Unfolding of case II_1 opens a crossing window delimited by $T_\alpha^{(1)}$ and $T_\alpha^{(2)}$ in the sliding segment. There are disjoint sliding segments of opposite stability for all sufficiently small $\alpha \neq 0$ but no attractors are involved.

Case II_2 is perhaps the less trivial local bifurcation in planar Filippov systems. The quadratic tangent points $T_\alpha^{(1)}$ and $T_\alpha^{(2)}$ delimit a single sliding segment for all small α . This segment is stable for $\alpha < 0$ and unstable for $\alpha > 0$. Moreover, the sliding segment contains a pseudo-node P_α , which is stable for $\alpha < 0$ and unstable for $\alpha > 0$. Finally, by analyzing the local Poincaré return map defined on Σ outside the sliding segment, one can prove that a unique and stable *crossing cycle* L_α exists for $\alpha > 0$ (see [Filippov, 1988]). This cycle shrinks together with the sliding segment and disappears when α is positive and tends to zero. Thus, in terms of isolated invariant sets, a stable pseudo-node existing for negative α is substituted by an unstable pseudo-node and a stable crossing cycle. Therefore, this bifurcation can be called *supercritical pseudo-Hopf bifurcation*.

The system (9) with

$$f^{(1)}(x, \alpha) = \begin{pmatrix} -1 - x_1 \\ -x_1 \end{pmatrix},$$

$$f^{(2)}(x, \alpha) = \begin{pmatrix} 1 \\ \alpha - x_1 \end{pmatrix}, \quad H(x, \alpha) = x_2,$$

is a local topological normal form for the supercritical pseudo-Hopf bifurcation (case II_2).

The bifurcation diagram in the subcritical case, corresponding to the unstable pseudo-focus ($k_2 > 0$), can be obtained from the described one by reversing the direction of all orbits and changing the sign of the parameter.

Notice that a normal form for II_1 can be obtained from that for II_2 by reversing $f^{(1)}$, i.e. with

$$f^{(1)}(x, \alpha) = \begin{pmatrix} 1 + x_1 \\ x_1 \end{pmatrix},$$

and $f^{(2)}$ and H as above.

3.3. Collisions of pseudo-equilibria

When α varies, two pseudo-equilibria can collide and disappear via the standard saddle-node bifurcation, which can properly be called in this case a *pseudo-saddle-node bifurcation*. Figure 13 illustrates this bifurcation in the case of a stable sliding segment. We will re-encounter this bifurcation while dealing with bifurcations of sliding cycles in Sec. 4.2.1.

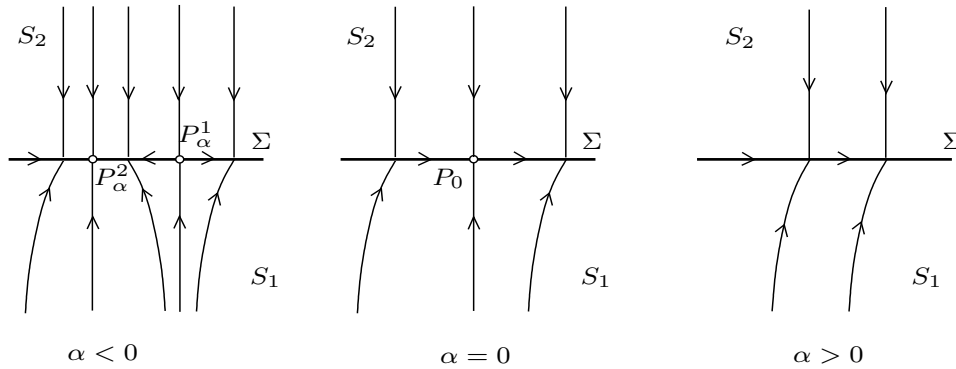


Fig. 13. Pseudo-saddle-node bifurcation.

A topological normal form for this bifurcation is (9), where

$$f^{(1)}(x, \alpha) = \begin{pmatrix} \alpha + x_1^2 \\ 1 \end{pmatrix},$$

$$f^{(2)}(x, \alpha) = \begin{pmatrix} 0 \\ -1 \end{pmatrix}, H(x) = x_2.$$

4. Global Bifurcations

4.1. Bifurcations of cycles

System (2) can have *standard periodic solutions* that lie entirely in S_1 or S_2 . All other periodic solutions can be naturally subdivided into two classes: periodic solutions which have a sliding segment in Σ (*sliding periodic solutions*) and those which have only isolated points in common with Σ (*crossing periodic solutions*). Note that a crossing periodic solution can pass through the boundary of the sliding segment. Accordingly, the orbits corresponding to periodic solutions will be called *standard*, *sliding* and *crossing cycles*. Due to uniqueness of forward solutions, sliding periodic solutions with a common sliding piece must coincide. One can introduce a local transversal section to a stable sliding cycle and define the Poincaré map in the usual way forward in time. However, the derivative of this map at the fixed point corresponding to the cycle will be zero, since all nearby points will be mapped into the fixed point. This is sometimes referred to as *superstability* and is related to the fact that the Poincaré map is noninvertible in this case. On the contrary, a generic crossing cycle has a smooth invertible Poincaré map and is exponentially stable if the derivative μ of the Poincaré map satisfies $\mu < 1$, and exponentially un-

stable if $\mu > 1$. Finally, a crossing cycle passing through the boundary of a sliding segment is superstable from both sides (see examples below).

Of course, sliding cycles can also cross Σ and have more than one sliding segment, while crossing cycles can return to Σ more than twice. In what follows we consider the simplest possible cycles and do not present state portraits that can be obtained from the considered ones by reversing all arrows.

4.1.1. Collision of a cycle with the boundary (touching)

A standard piece of a cycle can collide with the discontinuity boundary. This bifurcation is called *touching* or *grazing* or even the *sliding-grazing bifurcation*. The simplest case is that of a standard cycle that touches at $\alpha = 0$ a sliding segment Σ_s at a quadratic tangent point T_0 . Two generic critical cases ($TC_{1,2}$) are possible here, depending on the stability of the touching cycle L_0 from inside at $\alpha = 0$. In case TC_1 the cycle L_0 is stable from inside, while it is unstable from inside in case TC_2 .

The unfolding of TC_1 -singularity is presented in the upper part of Fig. 14. For $\alpha < 0$ there is a cycle $L_\alpha \subset S_1$ which is stable and which has the distance from Σ that is $O(\alpha)$ for small α . Then, for $\alpha > 0$, this cycle becomes a sliding cycle. Notice that stability of L_α changes from exponential stability to superstability.

The bifurcation diagram in case TC_2 is also shown in Fig. 14. For $\alpha > 0$ *two* cycles exist: An unstable cycle $L_\alpha^u \subset S_1$ and a sliding (superstable) cycle L_α . Since for $\alpha > 0$ no cycles remain, this bifurcation resembles the standard saddle-node bifurcation of limit cycles in smooth systems.

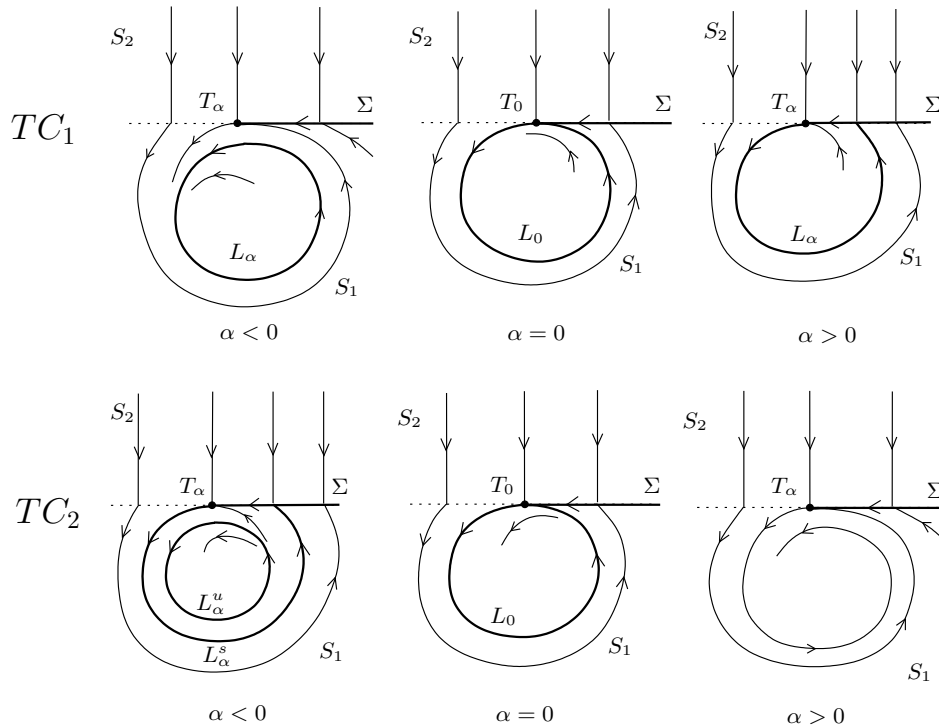


Fig. 14. Touching bifurcations.

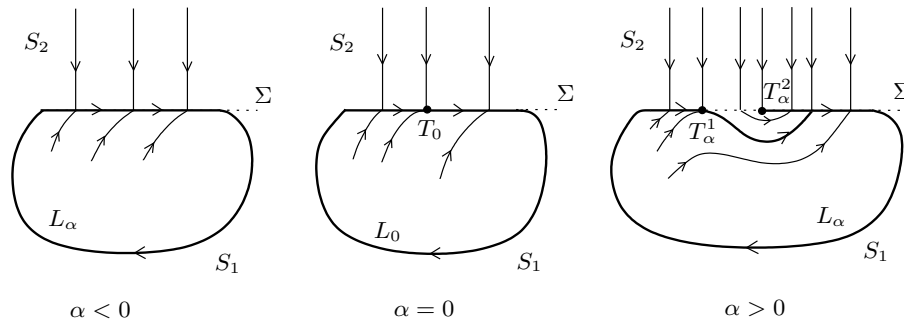


Fig. 15. Sliding disconnection.

4.1.2. *Appearance of a double tangency on the sliding cycle (sliding disconnection)*

Appearance of a double tangent point inside a sliding segment is a local bifurcation discussed in Sec. 3.2.1 (case DT_2). When this happens on a sliding cycle it causes a global change of the state portrait, depicted in Fig. 15. Assume that a sliding cycle L_α exists for $\alpha < 0$ and that a generic double tangent point T_0 appears in the sliding segment at $\alpha = 0$. For $\alpha > 0$, two visible quadratic tangent points, T_α^1 and T_α^2 , appear and interrupt the sliding motion, so that the cycle L_α now has two sliding

segments. Some authors call this rearrangement a *multi-sliding bifurcation*.

The following two bifurcations are purely global and are due to the collision of a sliding cycle with an invisible or visible quadratic tangent point.

4.1.3. *Return to an invisible tangent point (buckling)*

Assume that there exists a sliding cycle L_α for $\alpha < 0$ and that, for $\alpha = 0$ the standard piece of the cycle returns to the sliding segment at an invisible quadratic tangent point $T_0^{(1)}$ (see Fig. 16). If the

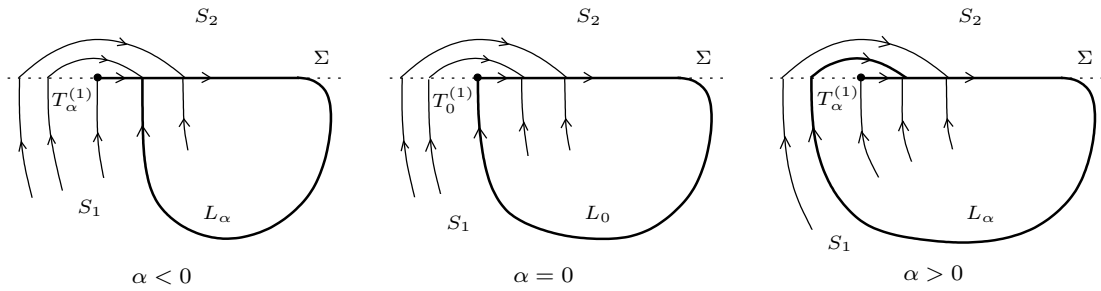


Fig. 16. Buckling bifurcation.

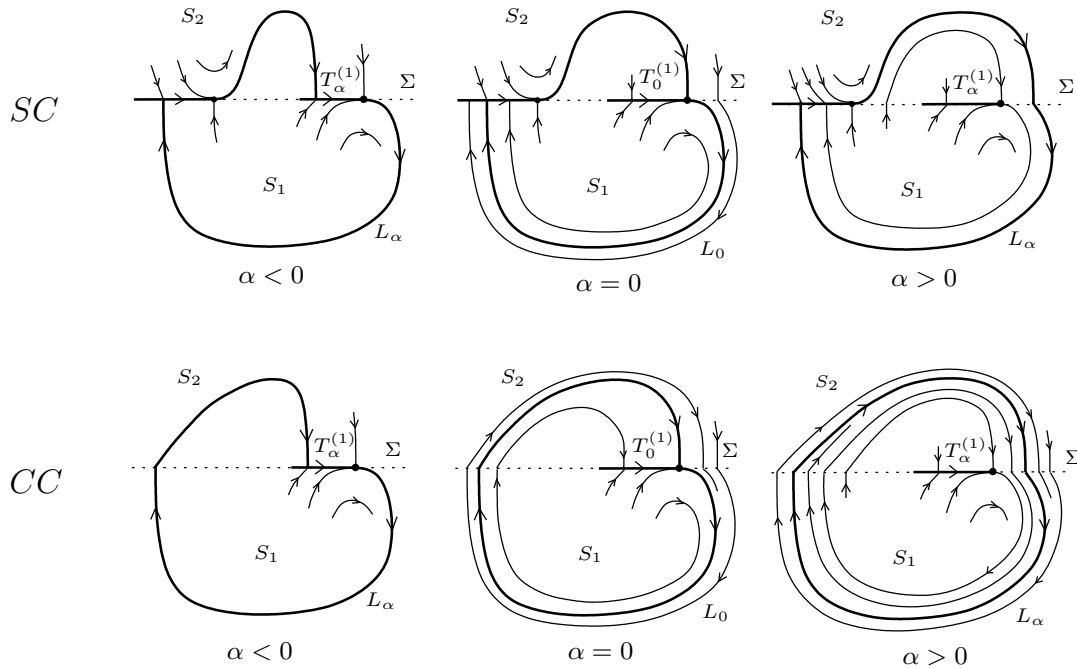


Fig. 17. Crossing bifurcations: *SC*: sliding critical cycle; *CC*: crossing critical cycle.

point of return of L_α on Σ passes with a nonzero velocity from the sliding to the crossing segment at $\alpha = 0$, then for $\alpha > 0$ the cycle remains but enters S_2 before returning back to the sliding segment. This is a *buckling bifurcation* of the sliding cycle (also called *sliding switching*).

4.1.4. *Return to a visible tangent point (crossing)*

The case of a periodic orbit starting at and returning to the same visible quadratic tangent point at $\alpha = 0$ is more complicated. Assuming genericity with respect to the parameter, there are two distinct cases as shown in Fig. 17. The critical cycle L_0 can be either sliding (case *SC*) or crossing (case *CC*).

Moreover, in both cases, it is superstable from inside and outside (see central portraits in Fig. 17). In all cases, there is a quadratic tangent point $T_\alpha^{(1)}$ of $f^{(1)}$ for all sufficiently small $|\alpha|$.

In case *SC*, a sliding cycle L_α with two sliding segments exists for $\alpha < 0$ and is substituted by a sliding cycle with only one sliding segment for $\alpha > 0$, since the orbit crosses Σ near $T_\alpha^{(1)}$. We call this bifurcation *simple crossing*.

In case *CC*, for $\alpha < 0$, there is a sliding cycle L_α with a single sliding segment ending at $T_\alpha^{(1)}$. This sliding segment shrinks for $\alpha \rightarrow 0$ and the cycle becomes for $\alpha = 0$, a crossing cycle that is superstable from both inside and outside. For $\alpha > 0$, a unique and exponentially stable

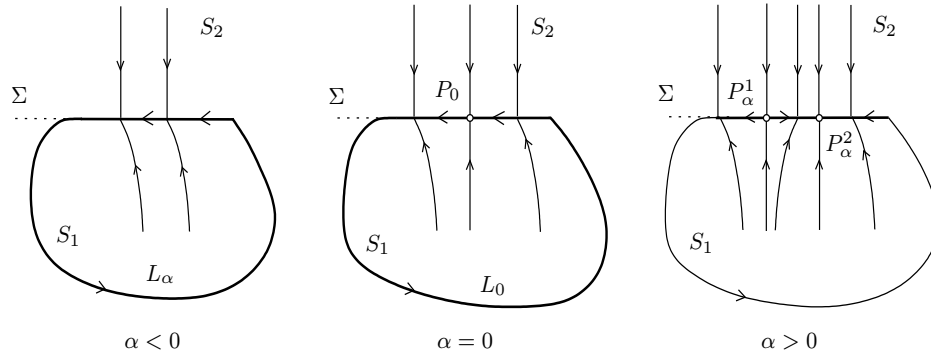


Fig. 18. Bifurcation of a homoclinic orbit to a pseudo-saddle-node.

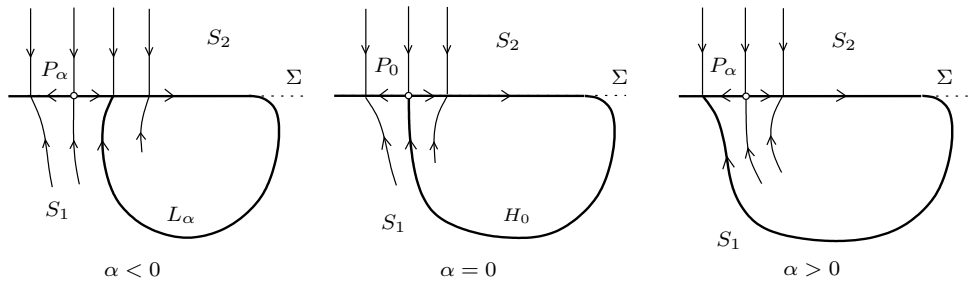


Fig. 19. Bifurcation of a sliding homoclinic orbit to a pseudo-saddle.

crossing cycle exists. Therefore, this bifurcation implies a transition from a superstable sliding cycle to an exponentially stable crossing cycle. We call it *sliding-crossing*.

In the last case CC_2 , a superstable sliding cycle L_α^s coexists with an exponentially unstable crossing cycle L_α^c for sufficiently small $\alpha < 0$. The two cycles collide at $\alpha = 0$ forming a critical crossing cycle L_0 and then disappear for $\alpha > 0$. This bifurcation, also called *sliding-crossing*, implies the catastrophic disappearance of a stable sliding cycle.

4.2. Pseudo-homoclinic bifurcations

A pseudo-equilibrium P_α of (7) can have a sliding orbit that starts and returns back to it at $\alpha = 0$. This is possible if P_0 is either a pseudo-saddle-node or a pseudo-saddle. Moreover, a standard saddle X_α can have a homoclinic orbit containing a sliding segment at $\alpha = 0$.

4.2.1. Sliding homoclinic orbit to a pseudo-saddle-node

Appearance of a pseudo-saddle-node inside a sliding segment is a local bifurcation discussed in

Sec. 3.3. If the pseudo-saddle-node appears on a sliding cycle L_α it causes a global change of the state portrait, as depicted in Fig. 18, where a sliding cycle L_α exists for $\alpha < 0$ and a generic pseudo-saddle-node P_0 appears in the sliding segment at $\alpha = 0$. Then, for $\alpha > 0$, a pseudo-saddle P_α^1 and a pseudo-node P_α^2 appear and interrupt the periodic motion, so that no cycle is present for $\alpha > 0$. All nearby orbits approach for small $\alpha > 0$ the stable pseudo-node P_α^2 . This bifurcation is completely analogous to the standard bifurcation of an orbit homoclinic to a saddle-node.

4.2.2. Sliding homoclinic orbit to a pseudo-saddle

A sliding cycle L_α can collide with a pseudo-saddle. Assuming that the orbit departing from a tangent point misses the pseudo-saddle transversally with respect to the parameter, we get the bifurcation diagram shown in Fig. 19, where a sliding cycle L_α exists for $\alpha < 0$ and becomes a sliding homoclinic orbit at $\alpha = 0$. There is no periodic orbit for $\alpha > 0$. This bifurcation is completely analogous to

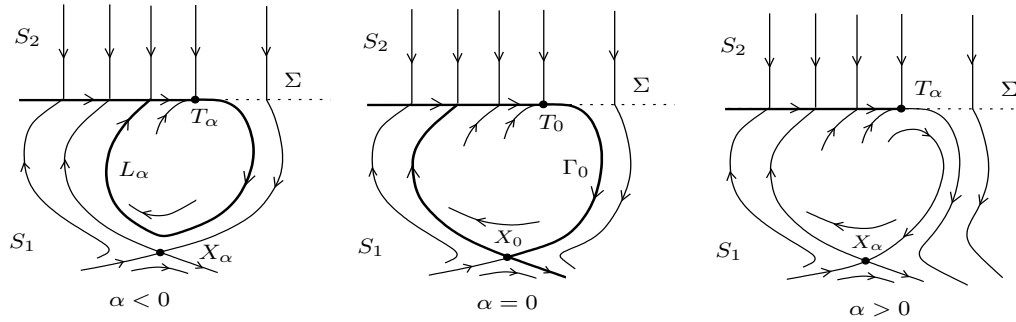


Fig. 20. Bifurcation of a sliding homoclinic orbit to a saddle.

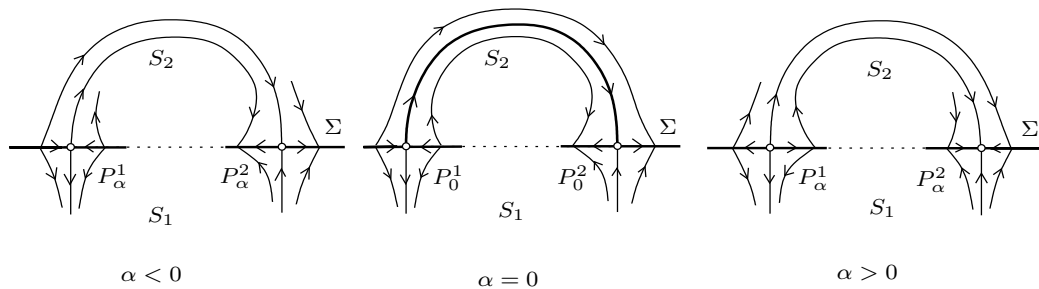


Fig. 21. Bifurcation of a heteroclinic orbit between pseudo-saddles.

the standard bifurcation of a homoclinic orbit to a saddle.

4.2.3. Sliding homoclinic orbit to a saddle

A sliding cycle L_α can collide with a standard saddle X_α , say in S_1 (see Fig. 20). Generically, the cycle existing for $\alpha < 0$ touches the saddle X_0 at $\alpha = 0$ and then disappears for $\alpha > 0$. This is another catastrophic bifurcation.

4.3. Pseudo-heteroclinic bifurcations

We complete our list of codim 1 global bifurcations, by considering also two rather simple possibilities related to heteroclinic orbits between pseudo-saddles and saddles. Note that there are also trivial bifurcations involving orbits which connect either two tangent points, or a special point with a pseudo-node. We do not present the corresponding diagrams here.

4.3.1. Heteroclinic connection between two pseudo-saddles

A generic unfolding of an orbit connecting two pseudo-saddles at $\alpha = 0$ is presented in Fig. 21.

For sufficiently small $|\alpha| \neq 0$, the heteroclinic connection breaks down giving rise to a bifurcation.

4.3.2. Heteroclinic connection between a pseudo-saddle and a saddle

A generic unfolding of an orbit connecting at $\alpha = 0$ a pseudo-saddle with a standard saddle in S_2 is given in Fig. 22. It does not involve nearby attractors and is listed here only for completeness.

5. Numerical Analysis of Bifurcations

One could consider (2) as the limit of a globally smooth system in \mathbf{R}^2 when some parameter $\varepsilon \rightarrow 0$. For example, one can define a smooth system

$$\dot{x} = S(x, \varepsilon)f^{(1)}(x) + (1 - S(x, \varepsilon))f^{(2)}(x), \quad (10)$$

where

$$S(x, \varepsilon) = \frac{1}{2} - \frac{1}{\pi} \arctan \left(\frac{H(x)}{\varepsilon} \right)$$

with $\varepsilon > 0$. Then, as $\varepsilon \rightarrow 0$, (10) tends toward the discontinuous system (2). Moreover, consider a forward solution $x(t)$ of (2) and suppose that it has no

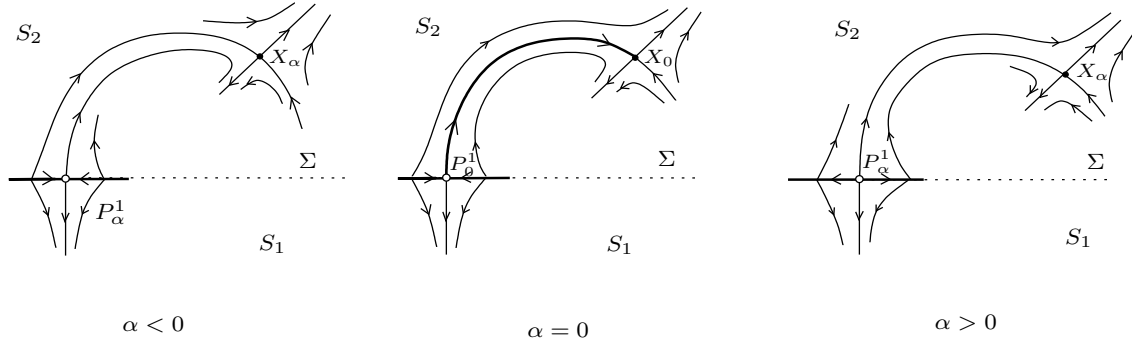


Fig. 22. Bifurcation of a heteroclinic orbit between a pseudo-saddle and a saddle.

unstable sliding segments. Then it can be proved that the solution $x_\varepsilon(t)$ of (10) with $x_\varepsilon(0) = x(0)$ tends to $x(t)$ uniformly on any finite time interval $[0, T]$.

Therefore, one could attempt to analyze the bifurcations of (10) using standard techniques for smooth ODEs [Doedel & Kernévez, 1986; Kuznetsov & Levitin, 1995–1997]. This is not easy, since (10) is a stiff ODE and, thus, requires special methods for its bifurcation analysis. But even worse than that, the most interesting sliding bifurcation phenomena are absent in (10). Thus, one has to develop special algorithms to deal with bifurcation analysis of Filippov systems. Below, we present such algorithms for the planar case, indicating, whenever possible, their applicability to the n -dimensional case.

5.1. One-parameter continuation

5.1.1. Continuation of pseudo-equilibria

A pseudo-equilibrium is an equilibrium of system (5) on the sliding manifold Σ_s . However, to set up equations for its continuation, which are valid in the n -dimensional case, it is more convenient to recall that at a pseudo-equilibrium x the vectors $f^{(1)}$ and $f^{(2)}$ are anti-collinear, namely

$$\lambda_1 f^{(1)}(x, \alpha) + \lambda_2 f^{(2)}(x, \alpha) = 0,$$

for some real λ_1 and λ_2 with $\lambda_1 \lambda_2 > 0$. This condition, together with the condition $H(x, \alpha) = 0$, gives the following defining system for the pseudo-equilibrium:

$$\begin{cases} H(x, \alpha) & = 0, \\ \lambda_1 f^{(1)}(x, \alpha) + \lambda_2 f^{(2)}(x, \alpha) & = 0, \\ \lambda_1 + \lambda_2 - 1 & = 0. \end{cases} \quad (11)$$

The system is valid for any $n \geq 2$. It is a system of $(n + 2)$ scalar equations in the $(n + 3)$ -dimensional space \mathbf{R}^{n+3} with coordinates (x, α, λ) . Generically, (11) defines a smooth one-dimensional manifold in \mathbf{R}^{n+3} , whose projection on the (x, α) -space gives a branch of pseudo-equilibria, provided $\lambda_1 \lambda_2 > 0$ and both $f^{(1)}$ and $f^{(2)}$ do not vanish.

If $\lambda_1 = 0$ at a point X but $\lambda_2 \neq 0$, then $f^{(2)}(X, \alpha) = 0$, i.e. X is an equilibrium of $f^{(2)}$ at the boundary Σ .

5.1.2. Continuation of tangent points

At a tangent point of $f^{(1)}$, the following two conditions are satisfied:

$$\begin{cases} H(x, \alpha) & = 0, \\ \langle H_x(x, \alpha), f^{(1)}(x, \alpha) \rangle & = 0. \end{cases} \quad (12)$$

Obviously, this system defines a curve only when the system is planar, since only in that case (12) is a system of two equations in the three-dimensional (x, α) -space. For three-dimensional Filippov systems, (12) defines a curve of tangent points in the state space \mathbf{R}^3 for a fixed parameter value α . A similar defining system can be specified for the tangent points of $f^{(2)}$.

5.1.3. Continuation of cycles

One might attempt to approximate the periodic solutions of a Filippov system with those of its smooth approximation (10) with sufficiently small $\varepsilon > 0$. Obviously, this approach does not work well near the discontinuity boundary. Indeed, if mesh adaptation is used, most of the mesh points accumulate near switches from standard to sliding motions.

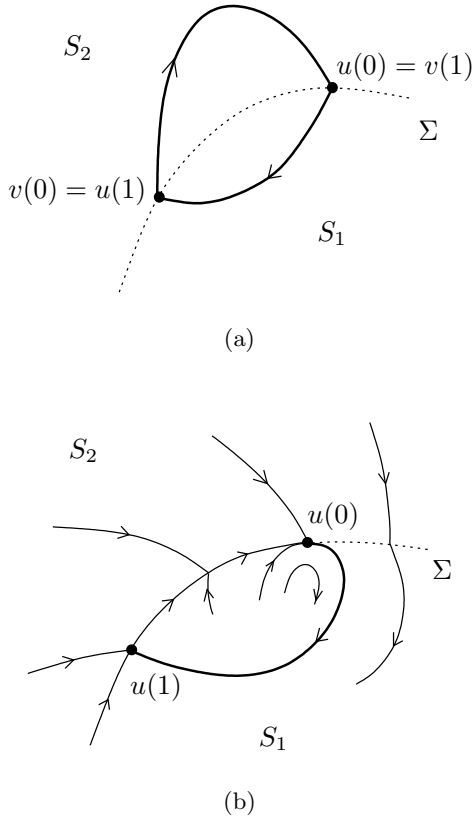


Fig. 23. The boundary-value problems for a crossing cycle (a) and a standard segment of a sliding cycle (b).

A simple countermeasure is to subdivide the periodic orbit into segments located entirely in S_1 or S_2 , and sliding segments. This approach works particularly well for the continuation of crossing cycles that cross Σ at only two points, $u(0)$ and $v(0)$ as shown in Fig. 23(a). Then the following boundary-value problem on the unit interval $[0, 1]$ can be used for the continuation of the crossing cycle:

$$\begin{cases} \dot{u} - T_1 f^{(1)}(u, \alpha) = 0, \\ H(u(0), \alpha) = 0, \\ u(1) - v(0) = 0, \\ \dot{v} - T_2 f^{(2)}(v, \alpha) = 0, \\ H(v(0), \alpha) = 0, \\ v(1) - u(0) = 0, \end{cases} \quad (13)$$

where T_i is a parameter meaning the time spent by the $(T_1 + T_2)$ -periodic solution in region S_i , $i = 1, 2$. The boundary conditions $u(1) = v(0)$ and $v(1) = u(0)$ ensure the periodicity, while the two scalar conditions involving H force the switch points to belong to the boundary Σ . The whole periodic

solution corresponding to the crossing cycle is then given by the formula:

$$x(t) = \begin{cases} u\left(\frac{t}{T_1}\right), & t \in [0, T_1], \\ v\left(\frac{t - T_1}{T_2}\right), & t \in [T_1, T_1 + T_2]. \end{cases}$$

Clearly, the approach is valid for any $n \geq 2$. A solution to the above boundary-value problem can be continued using the standard software AUTO97 [Doedel & Kernévez, 1986; Doedel *et al.*, 1997]. This is also true for all boundary-value problems discussed below.

The continuation of cycles with sliding segments is more complex. Indeed, the computation of such segments is equivalent to solving certain boundary-value problems for

$$\begin{cases} \dot{x} = g(x, \alpha), \\ 0 = H(x, \alpha), \end{cases} \quad (14)$$

where g is defined by a parameter-dependent analogue of (4). Note that (14) is a *differential-algebraic system* that can be numerically integrated using well-known codes, but for which boundary-value problem solvers are hard to develop (see, however, [Ascher & Spiteri, 1994]).

Fortunately, finding sliding periodic orbits in the planar case is much simpler, since the sliding segments coincide with pieces of the discontinuity boundary Σ , as shown in Fig. 23(b). Thus, the sliding segments can be computed for any fixed α by the continuation of the curve

$$H(x, \alpha) = 0,$$

and the problem is reduced to the continuation of the standard segment of the periodic orbit. As we have seen in the previous sections, generically, such a standard segment departs from Σ at a visible tangent point (in Fig. 23(b) $u(0)$ is a visible tangent point of $f^{(1)}$). After a finite-time T_1 (which is considered as a parameter), the orbit returns back to Σ at point $u(1)$. This means that the following boundary-value problem:

$$\begin{cases} \dot{u} - T_1 f^{(1)}(u, \alpha) = 0, \\ H(u(1), \alpha) = 0, \\ H(u(0), \alpha) = 0, \\ \langle H_x(u(0), \alpha), f^{(1)}(u(0), \alpha) \rangle = 0, \end{cases} \quad (15)$$

can be used to continue the standard segment located in S_1 . Notice that the last two equations in

(15) are nothing else than the defining equations (12) of the tangent point $u(0)$ of $f^{(1)}$.

5.2. Detection of bifurcations

To detect a bifurcation, a scalar *test function* ψ has to be constructed, which changes its sign at the bifurcation parameter value.

5.2.1. Test functions for local bifurcations

The most easily detectable local bifurcation is the collision of an equilibrium with the discontinuity boundary Σ (see Sec. 3.1). Indeed, following a standard equilibrium curve, say

$$f^{(1)}(x, \alpha) = 0,$$

one should merely monitor the test function

$$\psi_0(x, \alpha) = H(x, \alpha), \tag{16}$$

which has a regular zero when the equilibrium of $f^{(1)}$ hits Σ .

Other codim 1 local bifurcations occur within the discontinuity boundary. In particular, following a pseudo-equilibrium curve defined by (11), one can encounter the following codim 1 singularities:

- (1) collision with another pseudo-equilibrium;
- (2) collision with a boundary equilibrium.

These bifurcations can be detected, respectively, as zeroes of the test functions:

$$\psi_1(x, \alpha) = v_{n+1} \tag{17}$$

and

$$\psi_2(x, \alpha) = \lambda_1 \lambda_2, \tag{18}$$

where v_{n+1} is the α -component of the vector $v \in \mathbf{R}^{n+3}$ tangent to the curve defined by (11) at point (x, α, λ) .

Other codim 1 bifurcations in Σ can be detected by looking at tangent points. In particular, following a tangent point defined by (12) in a planar system, one can encounter two codim 1 singularities:

- (1) Double tangency of one vector field, say $f^{(1)}$, i.e. a visible and an invisible tangent points of $f^{(1)}$ collide;
- (2) Collision of tangent points of different vector fields, i.e. a tangent point of $f^{(1)}$ collides with a tangent point of $f^{(2)}$.

These bifurcations can be detected, respectively, as zeroes of the following test functions:

$$\psi_3(x, \alpha) = v_3, \tag{19}$$

and

$$\psi_4(x, \alpha) = \langle H_x(x, \alpha), f^{(2)}(x, \alpha) \rangle, \tag{20}$$

where v_3 is the α -component of the vector $v \in \mathbf{R}^3$ tangent to the curve defined by (12) at point (x, α) .

5.2.2. Detection of global bifurcations

Global bifurcations of sliding cycles caused by local events on a sliding segment, such as appearance of a double tangency (see Sec. 4.1.2) or appearance of a pseudo-saddle-node (see Sec. 4.2.1), can be detected by monitoring the local test functions described above.

Although some test functions could be constructed also for other global bifurcations described in Sec. 4, the most practical method to detect them is plotting orbits starting at visible tangent points and at pseudo-equilibria for different parameter values. We will return to the continuation of such global bifurcations later.

5.3. Two-parameter continuation of codim 1 bifurcations

In two-parameter families of Filippov systems, codim 1 bifurcations happen when we cross certain curves in the parameter plane. Here we construct *defining systems* which allow to compute such curves.

5.3.1. Continuation of local bifurcations

Obviously, the defining system

$$\begin{cases} f^{(1)}(x, \alpha) = 0, \\ H(x, \alpha) = 0, \end{cases} \tag{21}$$

can be used to continue a boundary equilibrium $x \in \mathbf{R}^n$ of $f^{(1)}$ with respect to two parameters, i.e. when $\alpha \in \mathbf{R}^2$.

The continuation of two coinciding tangent points of different vector fields is also straightforward in planar systems. Indeed, it is sufficient to add condition $\psi_4 = 0$ (see (20)) to system (12):

$$\begin{cases} H(x, \alpha) = 0, \\ \langle H_x(x, \alpha), f^{(1)}(x, \alpha) \rangle = 0, \\ \langle H_x(x, \alpha), f^{(2)}(x, \alpha) \rangle = 0. \end{cases} \tag{22}$$

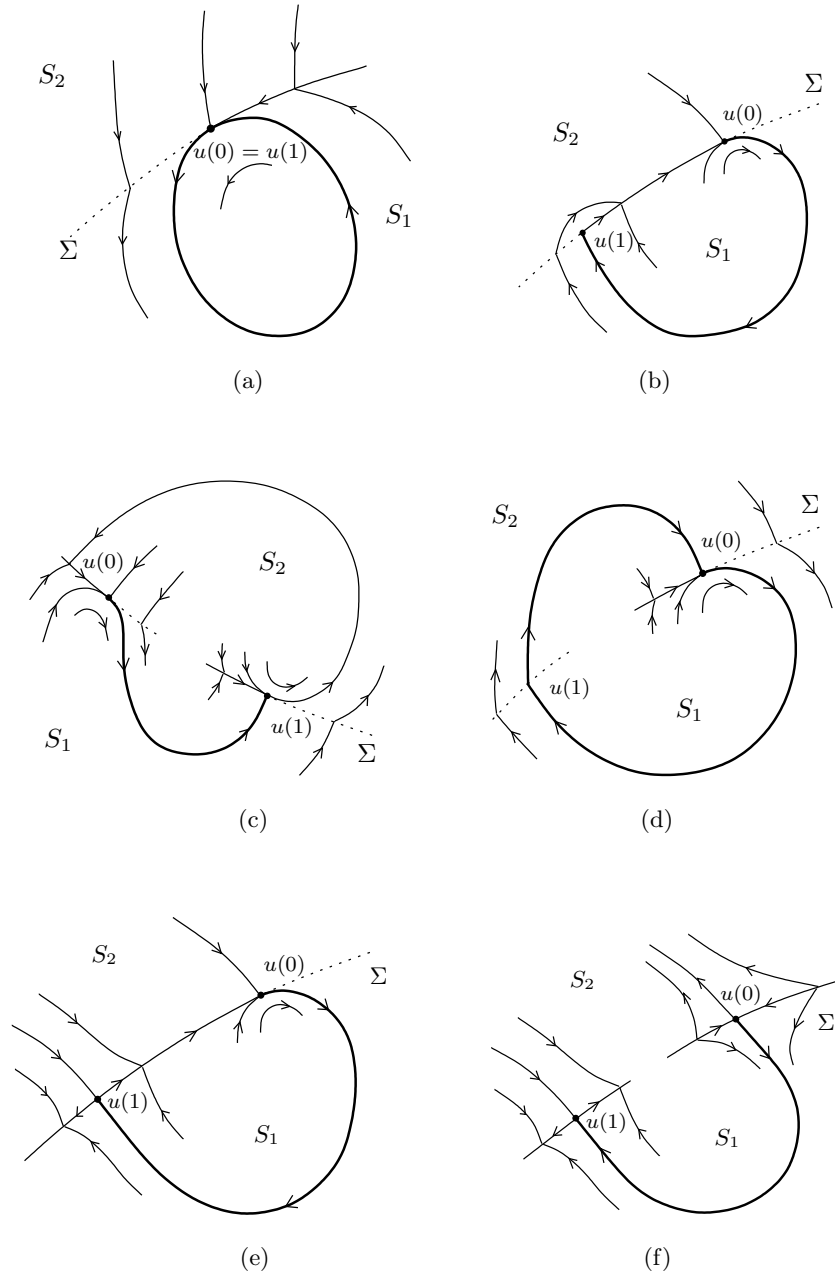


Fig. 24. The boundary-value problems for (a) touching bifurcation; (b) buckling bifurcation; (c) crossing bifurcation SC ; (d) crossing bifurcation CC ; (e) a homoclinic orbit to a pseudo-saddle; (f) an orbit connecting two pseudo-saddles.

The continuation of a double tangency of, say, $f^{(1)}$ with respect to two parameters is somehow more subtle. It can be done by adding to system (12) an extra equation

$$\frac{d^2}{dt^2} H(x(t), \alpha) \Big|_{t=0} = 0,$$

where $x(t)$ is the solution of $f^{(1)}$ starting at the

tangent point. Thus, the defining system

$$\begin{cases} H(x, \alpha) & = 0, \\ \langle H_x(x, \alpha), f^{(1)}(x, \alpha) \rangle & = 0, \\ \langle H_{xx}(x, \alpha) f^{(1)}(x, \alpha) & \\ + [f_x^{(1)}(x, \alpha)]^T H_x(x, \alpha), f^{(1)}(x, \alpha) \rangle & = 0, \end{cases} \quad (23)$$

is suitable for the two-parameter continuation of the double tangent point.

Finally, consider the two-parameter continuation of a pseudo-saddle-node (see Sec. 3.3). At a pseudo-saddle-node, the $(n + 2) \times (n + 2)$ Jacobian matrix of (11) with respect to $(x, \lambda_1, \lambda_2)$

$$J(x, \alpha, \lambda) = \begin{pmatrix} H_x^T & 0 & 0 \\ \lambda_1 f_x^{(1)} + \lambda_2 f_x^{(2)} & f^{(1)} & f^{(2)} \\ 0 & 1 & 1 \end{pmatrix}$$

has a nontrivial null-vector $v = (w, \mu_1, \mu_2)^T \in \mathbf{R}^{n+2}$: $Jv = 0$. Thus, the system

$$\begin{cases} H(x, \alpha) & = 0, \\ \lambda_1 f^{(1)}(x, \alpha) + \lambda_2 f^{(2)}(x, \alpha) & = 0, \\ \lambda_1 + \lambda_2 - 1 & = 0, \\ \langle H_x(x, \alpha), w \rangle & = 0, \\ \lambda_1 f_x^{(1)} w + \lambda_2 f_x^{(2)} w + \mu_1 f^{(1)} + \mu_2 f^{(2)} & = 0, \\ \mu_1 + \mu_2 & = 0, \\ \langle w, w \rangle + \mu_1^2 + \mu_2^2 - 1 & = 0, \end{cases} \quad (24)$$

can be used for the two-parameter continuation of a pseudo-saddle-node. This is a system of $(2n + 5)$ scalar equations in the $(2n + 6)$ -dimensional space with coordinates $(x, \alpha, \lambda, w, \mu)$. Obviously, (24) is valid in the general n -dimensional case.

5.3.2. Continuation of global bifurcations

Continuing global bifurcations with respect to two parameters is easier than detecting them, since all special points and orbits are already identified. Moreover, the continuation of a sliding disconnection (see Sec. 4.1.2) is equivalent to that of a double tangency, while the continuation of a sliding homoclinic orbit to a pseudo-saddle-node is equivalent to the continuation of the pseudo-saddle-node itself. These problems have been already considered in the previous subsection.

The two-parameter continuation of the touching bifurcation (see Sec. 4.1.1) of a cycle located in S_1 can be performed using the equations

$$\begin{cases} \dot{u} - T_1 f^{(1)}(u, \alpha) & = 0, \\ u(0) - u(1) & = 0, \\ H(u(0), \alpha) & = 0, \\ \langle H_x(u(0), \alpha), f^{(1)}(u(0), \alpha) \rangle & = 0. \end{cases} \quad (25)$$

Recall that T_1 is an extra parameter. This defining system can be derived by imposing $u(0) = u(1)$ in

(15) [cf. Figs. 23(b) and 24(a)]. This system is valid for $n \geq 2$.

By contrast, buckling (see Sec. 4.1.3) and SC -crossing (see Sec. 4.1.4) bifurcations are planar-specific. Indeed, both bifurcations are characterized by the condition that a standard segment of a cycle returns to Σ at a tangent point. Thus, for example, the following defining system (see Fig. 24(b), where $u(0)$ and $u(1)$ are a visible and an invisible tangent point of $f^{(1)}$, respectively) allows one to continue the buckling bifurcation:

$$\begin{cases} \dot{u} - T_1 f^{(1)}(u, \alpha) & = 0, \\ H(u(0), \alpha) & = 0, \\ H(u(1), \alpha) & = 0, \\ \langle H_x(u(0), \alpha), f^{(1)}(u(0), \alpha) \rangle & = 0, \\ \langle H_x(u(1), \alpha), f^{(2)}(u(1), \alpha) \rangle & = 0, \end{cases} \quad (26)$$

where T_1 is an extra parameter. The same defining system can be used for the continuation of a crossing bifurcation in the case of a sliding critical cycle (see Fig. 24(c), where $u(1)$ is a visible tangent point of $f^{(2)}$).

In order to continue a crossing critical cycle (see Fig. 24(d)) with respect to two parameters, a defining system should specify both standard segments (located in S_1 and S_2) of the critical cycle. If the critical cycle starts at a visible tangent point $u(0)$ of $f^{(1)}$, then it crosses the discontinuity boundary Σ at a point $u(1) = v(0)$ and proceeds in S_2 until it hits Σ again at $v(1) = u(0)$. Thus, the defining system takes the form:

$$\begin{cases} \dot{u} - T_1 f^{(1)}(u, \alpha) & = 0, \\ H(u(0), \alpha) & = 0, \\ u(1) - v(0) & = 0, \\ \dot{v} - T_2 f^{(2)}(v, \alpha) & = 0, \\ H(v(0), \alpha) & = 0, \\ v(1) - u(0) & = 0, \\ \langle H_x(u(0), \alpha), f^{(1)}(u(0), \alpha) \rangle & = 0, \end{cases} \quad (27)$$

where $T_{1,2}$ are parameters.

The remaining global bifurcations involve homoclinic and heteroclinic orbits to standard or pseudo-saddles. A sliding homoclinic orbit to a pseudo-saddle (see Sec. 4.2.2) can be continued

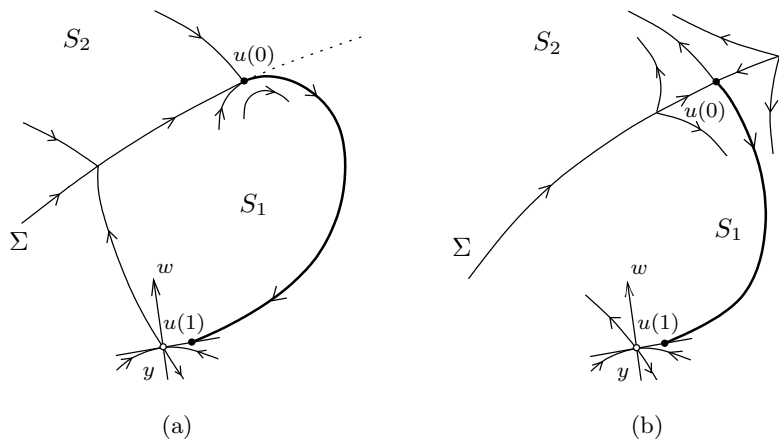


Fig. 25. The boundary-value problems for a sliding homoclinic orbit to a saddle (a) and an orbit connecting a pseudo-saddle to a saddle (b).

using the following defining system

$$\begin{cases} \dot{u} - T_1 f^{(1)}(u, \alpha) &= 0, \\ H(u(0), \alpha) &= 0, \\ \langle H_x(u(0), \alpha), f^{(1)}(u(0), \alpha) \rangle &= 0, \\ H(u(1), \alpha) &= 0, \\ \lambda_1 f^{(1)}(u(1), \alpha) + \lambda_2 f^{(2)}(u(1), \alpha) &= 0, \\ \lambda_1 + \lambda_2 - 1 &= 0. \end{cases} \quad (28)$$

Such a defining system can be easily derived by looking at Fig. 24(e), where the standard segment of the critical orbit is located in S_1 and connects a visible tangent point $u(0)$ of $f^{(1)}$ with a pseudo-saddle $u(1)$. The continuation of a solution to the boundary-value problem (28) will give a parameterization of the standard segment $u(\tau)$, $\tau \in [0, 1]$ in S_1 , the time T_1 spent by the standard orbit in S_1 , as well as the coordinates of the tangent point $u(0)$ and the pseudo-saddle $u(1)$ with its corresponding $\lambda_{1,2}$.

Similar defining functions can be used for the continuation of a standard orbit connecting two pseudo-saddles in a planar Filippov system (see Sec. 4.3.1 and Fig. 24(f)):

$$\begin{cases} \dot{u} - T_1 f^{(1)}(u, \alpha) &= 0, \\ H(u(0), \alpha) &= 0, \\ \lambda_1 f^{(1)}(u(0), \alpha) + \lambda_2 f^{(2)}(u(0), \alpha) &= 0, \\ \lambda_1 + \lambda_2 - 1 &= 0, \\ H(u(1), \alpha) &= 0, \\ \mu_1 f^{(1)}(u(1), \alpha) + \mu_2 f^{(2)}(u(1), \alpha) &= 0, \\ \mu_1 + \mu_2 - 1 &= 0. \end{cases} \quad (29)$$

All segments we have continued until now correspond to finite time intervals $T_{1,2}$, which were

treated as extra parameters in the boundary-value problems above. However, this is not the case when an orbit is asymptotic to a standard saddle. We have listed two such bifurcations: A heteroclinic connection between a pseudo-saddle and a standard saddle (Sec. 4.3.2) and a sliding homoclinic orbit to a saddle (Sec. 4.2.3). In both cases, one can employ the so-called *projection boundary conditions* at the standard saddle (see, for example, [Kuznetsov, 1998]) and truncate the boundary-value problem to a large but fixed time interval, namely require that an approximating orbit segment ends at a point of the stable linear subspace of the saddle, which is very close to the saddle itself. In the planar case, this can be formulated in terms of orthogonality to the adjoint unstable eigenvector.

For example, for the case of a sliding homoclinic orbit to a saddle depicted in Fig. 25(a) where $u(0)$ is a tangent point of $f^{(1)}$, y is a standard saddle in S_1 , and w is its adjoint eigenvector corresponding to the eigenvalue $\nu > 0$, the defining system takes the form:

$$\begin{cases} \dot{u} - T_1 f^{(1)}(u, \alpha) &= 0, \\ H(u(0), \alpha) &= 0, \\ \langle H_x(u(0), \alpha), f^{(1)}(u(0), \alpha) \rangle &= 0, \\ f^{(1)}(y, \alpha) &= 0, \\ [f_x^{(1)}(y, \alpha)]^T w - \nu w &= 0, \\ \langle w, w \rangle - 1 &= 0, \\ \langle w, y - u(1) \rangle &= 0, \end{cases} \quad (30)$$

where sufficiently large $T_1 > 0$ is fixed.

Similarly, for the two-parameter continuation of the heteroclinic connection between a

pseudo-saddle and a standard saddle shown in Fig. 25(b) one obtains the following defining system:

$$\begin{cases} \dot{u} - T_1 f^{(1)}(u, \alpha) & = 0, \\ H(u(0), \alpha) & = 0, \\ \lambda_1 f^{(1)}(u(0), \alpha) + \lambda_2 f^{(2)}(u(0), \alpha) & = 0, \\ \lambda_1 + \lambda_2 - 1 & = 0, \\ f^{(1)}(y, \alpha) & = 0, \\ [f_x^{(1)}(y, \alpha)]^T w - \nu w & = 0, \\ \langle w, w \rangle - 1 & = 0, \\ \langle w, y - u(1) \rangle & = 0, \end{cases} \quad (31)$$

with a big fixed $T_1 > 0$.

6. Example: Harvesting a Prey–Predator Community

In order to avoid the extinction of a valuable resource, exploitation is often forbidden when the resource is scarce. In this context, the simplest case of interest is that of a two population community (prey and predator with densities x_1 and x_2 , respectively), where the predator population is harvested only when abundant, i.e. when $x_2 > \alpha$, where α is a prescribed threshold. The standard Rosenzweig–MacArthur prey–predator model presented in many books (see, for example, [Bazykin, 1998]) is the most obvious candidate for describing the dynamics of the two populations when $x_2 < \alpha$. In that model the prey population grows logistically in the absence of predator and each predator transforms the harvested prey into new bornes. More precisely, the model for $x_2 < \alpha$ is the following:

$$\dot{x} = f^{(1)}(x, \alpha), \quad (32)$$

where

$$f^{(1)}(x, \alpha) = \begin{pmatrix} x_1(1 - x_1) - \psi(x_1)x_2 \\ \psi(x_1)x_2 - dx_2 \end{pmatrix}$$

and

$$\psi(x_1) = \frac{ax_1}{b + x_1}$$

is the functional response of the predator, namely the amount of prey eaten by each predator in one unit of time.

When the predator population is abundant ($x_2 > \alpha$) an extra mortality must be added to the second equation in order to take exploitation into account. If we assume that the resource is exploited

at constant effort E , the equation for $x_2 > \alpha$ takes the form

$$\dot{x} = f^{(2)}(x, \alpha), \quad (33)$$

where

$$f^{(2)}(x, \alpha) = \begin{pmatrix} x_1(1 - x_1) - \psi(x_1)x_2 \\ \psi(x_1)x_2 - dx_2 - Ex_2 \end{pmatrix}.$$

Since the prey equation is the same in both regions $S_1 = \{x : x_2 < \alpha\}$ and $S_2 = \{x : x_2 > \alpha\}$, there is a unique nontrivial zero-isocline $\dot{x}_1 = 0$, which is the parabola

$$x_2 = \frac{1}{a}(b + x_1)(1 - x_1). \quad (34)$$

By contrast, the nontrivial zero-isoclines $\dot{x}_2 = 0$ are different in the two regions. More precisely, they are vertical straight lines given by

$$x_1 = \frac{bd}{a - d}, \quad x \in S_1,$$

and

$$x_1 = \frac{b(d + E)}{a - (d + E)}, \quad x \in S_2.$$

From this it follows that there are two distinct tangent points $T^{(1)}$ and $T^{(2)}$ given by the intersections of the horizontal discontinuity boundary $\Sigma = \{x : x_2 = \alpha\}$ with the two zero-isoclines. The horizontal segment between the tangent points is a sliding segment Σ_s and contains pseudo-equilibria if it intersects the parabola (34). In fact, at these intersection points the tangent vectors \dot{x} are vertical and anti-collinear (condition for pseudo-equilibrium). The bifurcation analysis with respect to α is therefore relatively easy and can be performed analytically in great part.

In Figs. 26 and 27 we show the results of this analysis for the following values of the parameters: $a = 0.3556$, $b = 0.33$, $d = 0.0444$, $E = 0.2067$.

Figure 26 presents generic state portraits corresponding to different decreasing values of α , while intermediate critical state portraits are plotted in Fig. 27. All together, there are five different bifurcations. The first [Fig. 27(a)] is a touching bifurcation (see Sec. 4.1.1), where the classical prey–predator limit cycle [Fig. 26(a)] becomes a sliding cycle [Fig. 26(b)]. The second [Fig. 27(b)] is a pseudo-saddle-node bifurcation (see Sec. 3.3): It generates a pseudo-saddle and a stable pseudo-node [Fig. 26(c)]. Just after that bifurcation, there are two attractors: the stable pseudo-node and the stable sliding cycle. The third bifurcation is

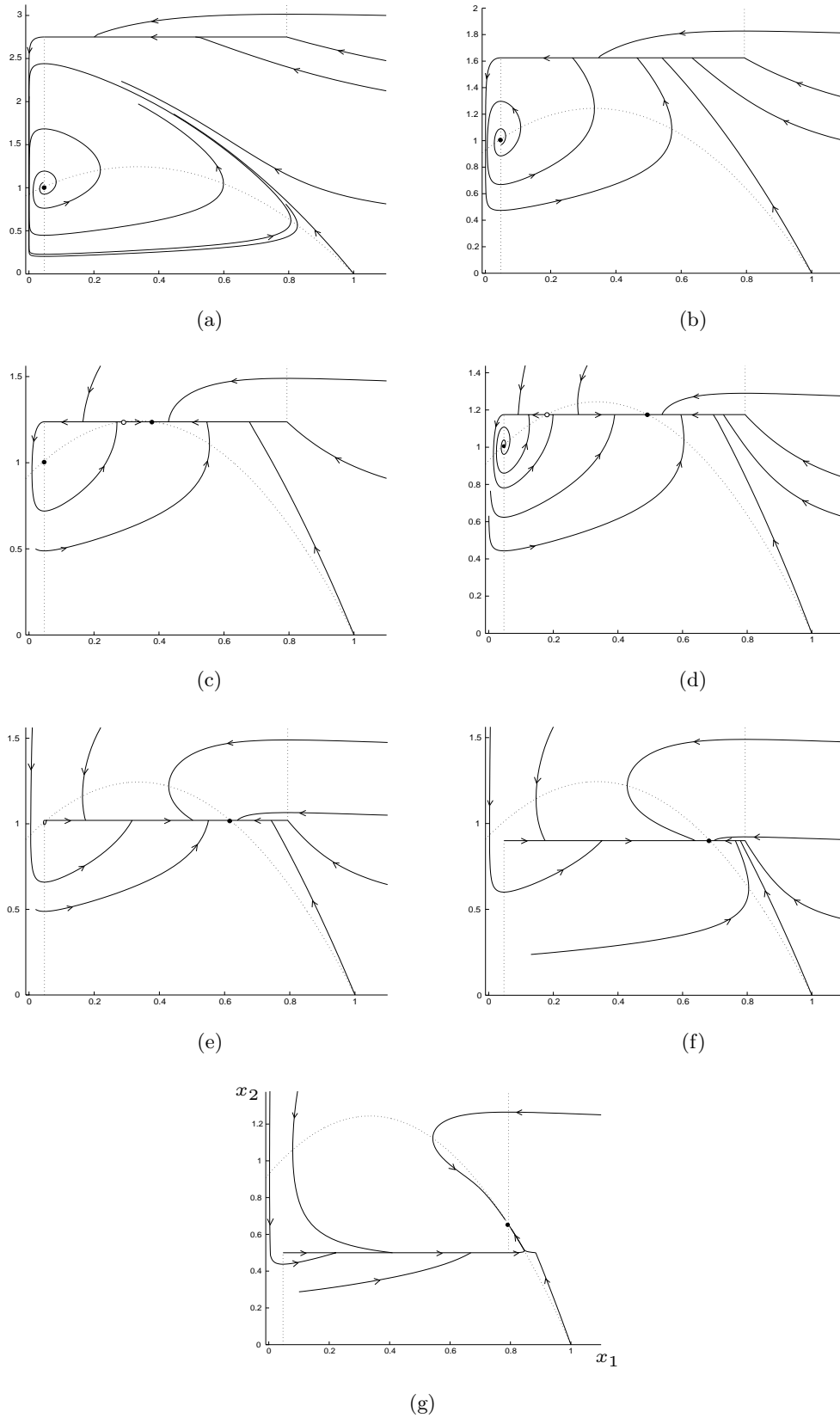


Fig. 26. Generic state portraits of model (32)–(33): (a) a stable standard cycle at $\alpha = 2.75$; (b) a stable sliding cycle at $\alpha = 1.625$; (c) a stable sliding cycle and a stable pseudo-node at $\alpha = 1.2375$; (d) a stable pseudo-node at $\alpha = 1.175$; (e) a stable sliding cycle (almost invisible) and a stable pseudo-node at $\alpha = 1.02$; (f) a stable pseudo-node at $\alpha = 0.9$; (g) a stable standard node at $\alpha = 0.5$.

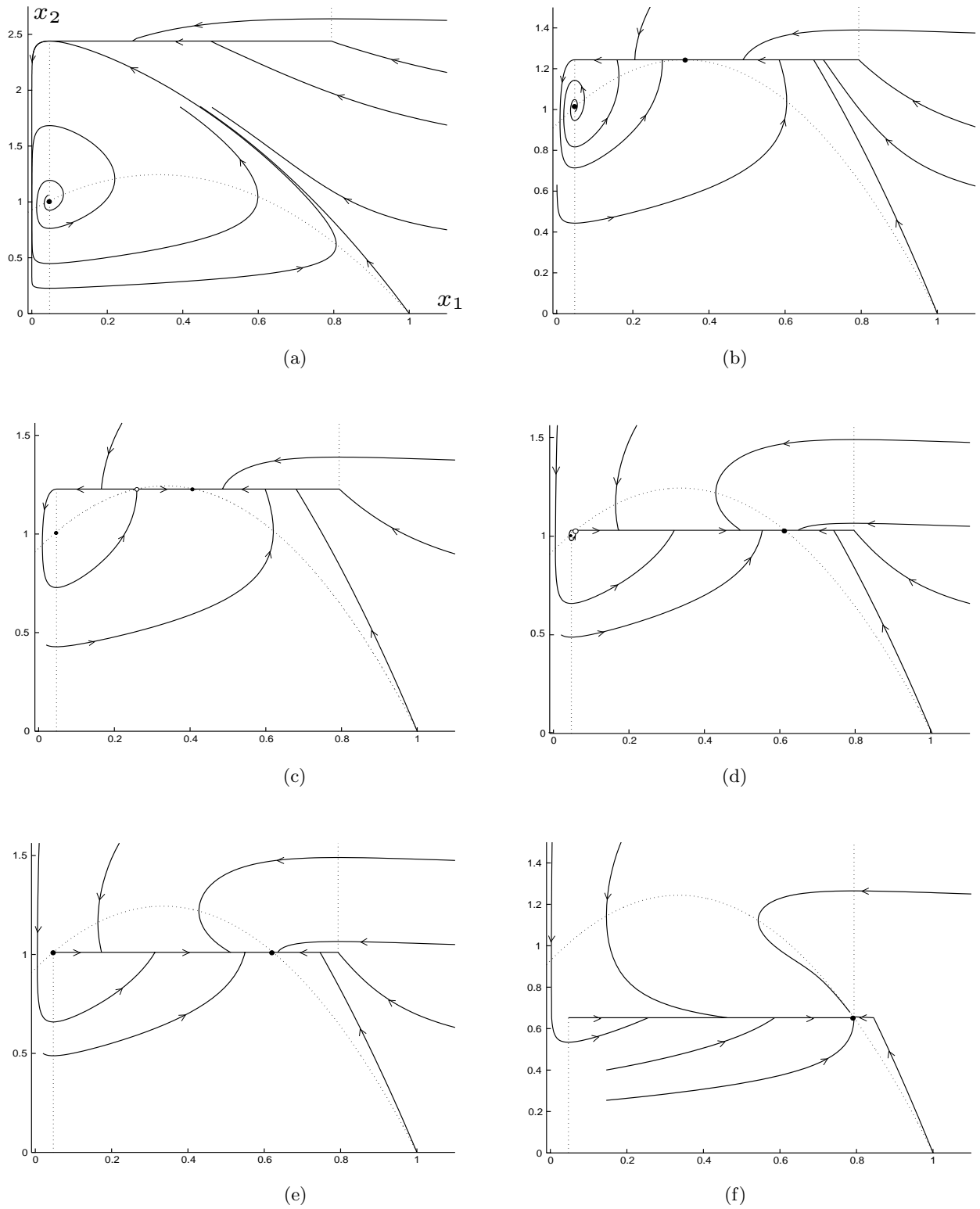


Fig. 27. Critical state portraits of model (32), (33): (a) Touching bifurcation at $\alpha \approx 2.440$; (b) pseudo-saddle-node bifurcation at $\alpha \approx 1.2437$; (c) sliding homoclinic orbit to a pseudo-saddle bifurcation at $\alpha \approx 1.2277$; (d) another sliding homoclinic orbit to a pseudo-saddle (almost invisible) at $\alpha \approx 1.03$; (e) boundary focus bifurcation at $\alpha \approx 1.01017$; (f) boundary node bifurcation at $\alpha \approx 0.6527$.

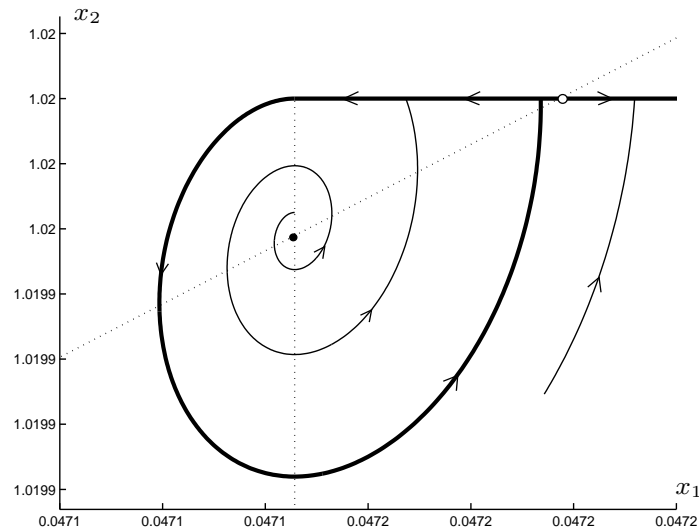


Fig. 28. Magnification of a small sliding cycle at $\alpha = 1.02$.

a global bifurcation characterized by the presence of a sliding homoclinic orbit to the pseudo-saddle [Fig. 27(c)]. After this bifurcation the sliding cycle does not exist and the stable pseudo-node remains the only attractor [Fig. 26(d)]. The fourth bifurcation [Fig. 27(d)] is due to another sliding homoclinic orbit to the pseudo-saddle, after which the sliding cycle reappears but has a much smaller size (see Figs. 26(e) and 28 for a magnification). The fifth bifurcation [Fig. 27(e)] is a boundary focus bifurcation (see case BF_1 in Sec. 3.1.1), where the small sliding cycle shrinks and disappears. For lower threshold values the attractor is again unique, namely a stable pseudo-node [Fig. 26(f)], which becomes a stable node [Fig. 26(f)] after the last bifurcation [Fig. 27(f)], which is a boundary node bifurcation (case BN_1 in Sec. 3.1.1).

The state portraits in Fig. 26 are interesting: They show that high degrees of protectionism (high threshold values α) allow the ecosystem to behave cyclically with very large excursions of prey and predator populations. Lower threshold values, i.e. reasonable degrees of protectionism, prevent the periodic and dangerous crashes of the predator population. However, for these threshold values the ecosystem can have two attractors. Finally, for very low protectionism the ecosystem is at the exploited equilibrium, characterized by a low predator density. The most striking result of this bifurcation analysis is that the discontinuous exploitation introduced with the threshold has the

power of creating multiple attractors [see Figs. 26(c) and 26(e)], which, indeed, are not possible in the standard Rosenzweig–MacArthur model. A deeper understanding of the dynamics of discontinuously exploited ecosystems requires a bifurcation analysis also with respect to more than one parameter. This can be done by continuation using the defining functions described in Sec. 5. Such computations have been done with respect to b and α (see Fig. 29). Details of this analysis and a complete bifurcation diagram of (32)–(33) will be reported elsewhere.

7. Discussion

We have presented an overview of all one-parameter bifurcations in generic planar discontinuous piecewise smooth autonomous systems (here called Filippov systems). Apart from numerous applications, there are two natural directions in which the analysis presented in this paper can be extended: to more dimensions and to higher codimensions.

As we have already mentioned in the Introduction, there is a growing number of interesting results on bifurcations of periodic solutions in specific three-dimensional and in general n -dimensional Filippov systems (see, for example [Feigin, 1994; di Bernardo *et al.*, 1999; di Bernardo *et al.*, 1998; di Bernardo *et al.*, 1998; di Bernardo *et al.*, 2001], and, in particular, [di Bernardo *et al.*, 2002]). Much less is known about local bifurcations in n -dimensional systems. Filippov [1988] has identified codim 1 boundary equilibria and tangent

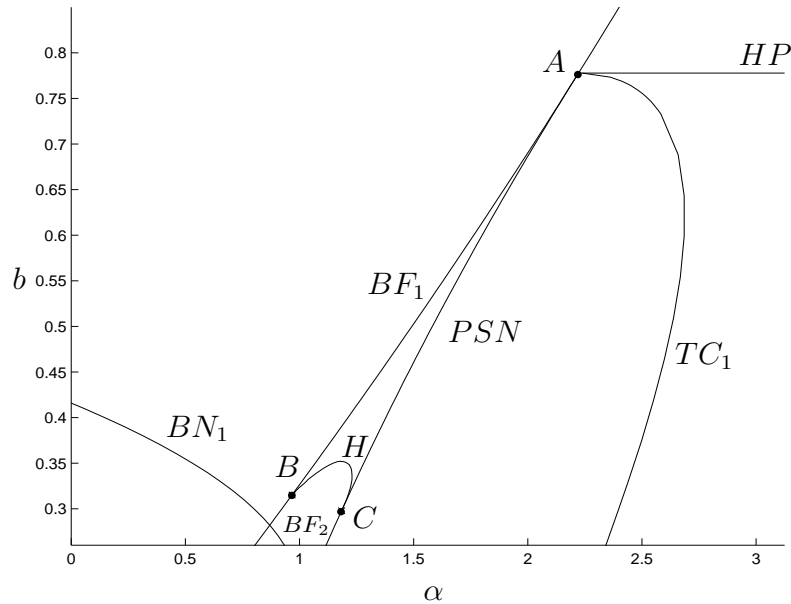


Fig. 29. Bifurcation diagram of model (32)–(33) in the (α, b) -plane for $b > 0.26$. The dotted line corresponds to the one-parameter family with $b = 0.33$. Bifurcation curves: HP — standard Hopf bifurcation; $BF_{1,2}$ — boundary foci; BN_1 — boundary node; PSN — pseudo saddle-node; TC_1 — touching; H — sliding homoclinic orbit to a pseudo-saddle. Points of codim 2 bifurcations: A — boundary Hopf bifurcation; B — degenerate boundary focus; C — sliding homoclinic orbit to a pseudo-saddle-node.

points in three-dimensional systems. Unfortunately, his classification should be done from scratch for each dimension n , since the dimension of the set of tangent points is equal to $n - 2$ and thus depends on n . If no tangent points are involved, the situation is relatively easy and one can apply standard bifurcation theory to pseudo-equilibria within the sliding set Σ_s . In generic one-parameter families of Filippov systems, only fold and Hopf bifurcations of pseudo-equilibria occur within Σ_s . In the case of fold bifurcation, two pseudo-equilibria appear or disappear at the bifurcation parameter value. The Hopf case implies the appearance or disappearance of a small periodic orbit in the sliding manifold. The existence of tangent points makes the bifurcation picture more complicated, since no center manifold reduction is possible. However, many local codim 1 bifurcations involving tangent curves and sliding are most likely treatable for $n = 3$.

The analysis of codim 2 local bifurcations in planar Filippov systems seems feasible. Notice that two such points are present in Fig. 29: A — a standard Hopf bifurcation occurring at the discontinuity boundary (boundary Hopf), and B — a degenerate boundary focus satisfying condition (8) from Sec. 3.1.1. Generic two-parameter unfoldings of these singularities will have bifurcation

diagrams similar to those near points A and B in Fig. 29. However, many more codim 2 bifurcations are present even in model (32)–(33). Another interesting codim 2 case is a degenerate pseudo-Hopf bifurcation, where $k_2 = 0$ (see Secs. 2.2 and 3.2.4). Its two-parameter unfolding has a curve where two crossing cycles of opposite stability collide and disappear.

There are other interesting topics, related to the numerical analysis of n -dimensional Filippov systems. For example, it would be interesting to analyze rearrangements of one- (and, eventually, two-parameter) bifurcation diagrams of smooth systems defined by (10), when $\varepsilon \rightarrow 0^+$, and understand how these diagrams tend to the diagrams of the corresponding discontinuous systems. This seems to be a nontrivial problem, since there are obviously no sliding motions in (10) for any $\varepsilon > 0$. Asymptotic methods from the theory of singularly perturbed ODEs might be applicable to that problem. Among others, the problem of the continuation of sliding cycles in n -dimensional Filippov systems as solutions of certain boundary-value problems for differential-algebraic equations, is the most challenging one. Recall, however, that the continuation of the grazing bifurcation (see Sec. 4.1.1) can be done using system (25) for all $n \geq 2$.

Acknowledgments

The authors are grateful to F. Dercole (Politecnico di Milano, Italy) for critical and constructive comments on an early draft of this paper. We would also like to thank U. Galvanetto (Imperial College of Science, Technology and Medicine, London, UK) and A. Nordmark (Royal Institute of Technology, Stockholm, Sweden) for spotting errors in our original classification of global sliding bifurcations.

References

- Ascher, U. M. & Spiteri, R. J. [1994] “Collocation software for boundary value differential-algebraic equations,” *SIAM J. Sci. Comput.* **15**, 938–952.
- Aubin, J. P. & Cellina, A. [1984] *Differential Inclusions* (Springer-Verlag, Berlin).
- Bautin, N. N. & Leontovich, E. A. [1976] *Methods and Techniques for Qualitative Analysis of Dynamical Systems on the Plane* (Nauka, Moscow), (in Russian).
- Bazykin, A. D. [1998] *Nonlinear Dynamics of Interacting Populations* (World Scientific, Singapore).
- Brogliato, B. [1999] *Nonsmooth Mechanics* (Springer-Verlag, NY).
- Dankowitz, H. & Nordmark, A. B. [2000] “On the origin and bifurcations of stick-slip oscillations,” *Physica D* **136**, 280–302.
- di Bernardo, M., Champneys, A. R. & Budd, C. J. [1998a] “Grazing, skipping and sliding: Analysis of the nonsmooth dynamics of the DC/DC buck converter,” *Nonlinearity* **11**, 858–890.
- di Bernardo, M., Garofalo, F., Glielmo, L. & Vasca, F. [1998b] “Switchings, bifurcations and chaos in DC/DC converters,” *IEEE Trans. Circuits Syst. I Fund. Th. Appl.* **45**, 133–143.
- di Bernardo, M., Feigin, M. I., Hogan, S. J. & Homer, M.E. [1999] “Local analysis of C-bifurcations in n -dimensional piecewise smooth dynamical systems,” *Chaos Solit. Fract.* **10**, 1881–1908.
- di Bernardo, M., Budd, C. J. & Champneys, A. R. [2001a] “Grazing and border-collision in piecewise-smooth systems: A unified analytical framework,” *Phys. Rev. Lett.* **86**, 2553–2556.
- di Bernardo, M., Johansson, K. H. & Vasca, F. [2001b] “Self-oscillations and sliding in relay feedback systems: Symmetry and bifurcations,” *Int. J. Bifurcation and Chaos* **11**, 1121–1140.
- di Bernardo, M., Kowalczyk, P. & Nordmark, A. [2002] “Bifurcations of dynamical systems with sliding: Derivation of normal-form mappings,” *Physica D* **11**, 175–205.
- Doedel, E. J. & Kernévez, J. P. [1986] “AUTO: Software for continuation problems in ordinary differential equations with applications,” Technical Report, California Institute of Technology, Applied Mathematics.
- Doedel, E. J., Champneys, A. R., Fairgrieve, T. F., Kuznetsov, Yu. A., Sandstede, B. & Wang, X. J. [1997] “AUTO97: Continuation and bifurcation software for ordinary differential equations (with HomCont), User’s Guide,” Technical Report, Concordia University, Montreal, Canada.
- Doole, S. H. & Hogan, S. J. [1996] “A piecewise linear suspension bridge model: Nonlinear dynamics and orbit continuation,” *Dyn. Stab. Syst.* **11**, 19–29.
- Feigin, M. I. [1994] *Forced Oscillations in Systems with Discontinuous Nonlinearities* (Nauka, Moscow), (in Russian).
- Filippov, A. F. [1964] “Differential equations with discontinuous right-hand side,” in *American Mathematical Society Translations*, Series 2, (AMS), pp 199–231.
- Filippov, A. F. [1988] *Differential Equations with Discontinuous Right-Hand Sides* (Kluwer Academic, Dordrecht).
- Flügge-Lotz, I. [1953] *Discontinuous Automatic Control* (Princeton University Press).
- Freire, E., Ponce, E., Rodrigo, F. & Torres, F. [1998] “Bifurcation sets of continuous piecewise linear systems with two zones,” *Int. J. Bifurcation and Chaos* **8**, 2073–2097.
- Galvanetto, U., Bishop, S. R. & Briseghella, L. [1995] “Mechanical stick-slip vibrations,” *Int. J. Bifurcation and Chaos* **5**, 651–673.
- Gatto, M., Mandrioli, D. & Rinaldi, S. [1973] “Pseudoequilibrium in dynamical systems,” *Int. J. Syst. Sci.* **4**, 809–824.
- Giannakopoulos, F. & Pliete, K. [2001] “Planar systems of piecewise linear differential equations with a line of discontinuity,” *Nonlinearity* **14**, 1–22.
- Gubar’, N. A. [1971] “Bifurcations in the vicinity of a ‘fused focus’,” *J. Appl. Math. Mech.* **35**, 890–895.
- Guckenheimer, J. & Holmes, P. [1983] *Nonlinear Oscillations, Dynamical Systems, and Bifurcations of Vector Fields* (Springer-Verlag, NY).
- Hasler, M. & Neiryneck, J. [1985] *Circuits Non Linéaires* (Presses Polytechniques Romandes, Lausanne).
- Hogan, S. J. [1989] “On the dynamics of rigid-block motion under harmonic forcing,” *Proc. Roy. Soc. London A* **425**, 441–476.
- Kowalczyk, P. & di Bernardo, M. [2001] “On a novel class of bifurcations in hybrid dynamical systems: The case of relay feedback systems,” in *Hybrid Systems: Computation and Control*, eds. di Benedetto, M. & Sangiovanni-Vincentelli, A. (Springer-Verlag, Berlin), pp. 361–374.
- Kunze, M. & Küpper, T. [1997] “Qualitative bifurcation analysis of a non-smooth friction oscillator model,” *Z. Angew. Math. Phys.* **48**, 87–101.
- Kunze, M. [2000] *Non-Smooth Dynamical Systems*, Lecture Notes in Mathematics, Vol. 1744, (Springer-Verlag, Berlin).

- Kuznetsov, Yu. A. & Levitin, V. V. [1995–1997] “CONTENT: A multiplatform environment for analyzing dynamical systems,” Technical Report, Dynamical Systems Laboratory, CWI, Amsterdam, The Netherlands. <ftp://ftp.cwi.nl/pub/CONTENT>.
- Kuznetsov, Yu. A. [1998] *Elements of Applied Bifurcation Theory*, 2nd edition (Springer-Verlag, NY).
- Leine, R. I. [2000] “Bifurcations in discontinuous mechanical systems of Filippov-type,” PhD thesis, Technical University of Eindhoven, The Netherlands.
- McGeer, T. [1990] “Passive dynamic walking,” *Int. J. Robot. Res.* **9**, 62–82.
- Oestreich, M., Hinrichs, N., Popp, K. & Budd, C. J. [1997] “Analytical and experimental investigation of an impact oscillator,” *Proc. ASME 16th Biennial Conf. Mech. Vibrations and Noise*, Sacramento, California, DETC97VIB-3907, 1–11.
- Tsytkin, Ya. Z. [1984] *Relay Control Systems* (Cambridge University Press).
- Utkin, V. I. [1977] “Variable structure systems with sliding modes,” *IEEE Trans. Automat. Contr.* **22**, 212–222.
- Van de Vrande, B. L., Van Campen, D. H. & De Kraker, A. [1999] “An approximate analysis of dry-friction-induced stick-slip vibration by a smoothing procedure,” *Nonlin. Dyn.* **19**, 157–169.